

DETERMINATION OF TARGET THICKNESS
OF THIN LITHIUM TARGETS

C. F. Donaghy

8854
on spine:

DONAGHY

1954

THESIS
D643

Letter on front cover:

DETERMINATION OF TARGET THICKNESS
OF THIN LITHIUM TARGETS

C. F. DONAGHY

8425
DETERMINATION OF TARGET THICKNESS
OF THIN LITHIUM TARGETS

by

C. F. Donaghy
Lieutenant, U. S. Navy

B.S., United States Naval Academy
(1944)

SUBMITTED IN PARTIAL FULFILLMENT OF THE
REQUIREMENTS FOR THE DEGREE OF
MASTER OF SCIENCE

at the

MASSACHUSETTS INSTITUTE OF TECHNOLOGY
(1954)

From

2643

RECEIVED DEPT. OF AGRICULTURE

WASHINGTON, D. C.

1914

March 1, 1914

Mr. J. H. ...

Washington, D. C.

[Signature]

RECEIVED DEPT. OF AGRICULTURE

WASHINGTON, D. C.

March 1, 1914

1914

RECEIVED DEPT. OF AGRICULTURE

DETERMINATION OF TARGET THICKNESS OF THIN LITHIUM TARGETS

C. F. Donaghy
Lieutenant, U. S. Navy

Submitted to the Department of Physics on May 24, 1954 in
partial fulfillment of the requirements for the degree of
Master of Science

A B S T R A C T

A study has been made of the mechanics leading to a geometric peak in the neutron yield curve of endoergic (p,n) reactions.

Theoretical expressions have been derived for the neutron yield as a function of proton energy and counter position for the case of a monoenergetic proton beam, assuming isotropic emission of neutrons in the center-of-mass system and neglecting proton straggling within the target. The derivative of the theoretical yield curve is evaluated at the peak position to get an equation for target thickness in terms of peak position, counter position, and reaction threshold. These results are applied to the $\text{Li}(p,n)$ reaction.

The effects of proton straggling and spread in the proton beam energy are then considered, and a method given to obtain an approximation to target thickness where these effects must be taken into account as is the case for very thin targets.

Thesis Supervisor: Clark Goodman
Title: Associate Professor of Physics

~~25008~~

28803

ACKNOWLEDGMENTS

The author* takes pleasure in expressing his appreciation to Dr. Robert Kiehn for suggesting this research problem and to Professor Clark Goodman, who supervised the work while in progress, for his optimism and encouragement throughout.

The author thanks Hans Mark for the many interesting discussions of this problem and related topics over the past year.

Mrs. William Guernsey and Clyde McClelland were both of material assistance in operating the generator. The unenviable task of typing the manuscript was excellently performed by Mrs. Mary E. White in a very limited amount of time, for which the author will always be grateful.

*Enrolled at the Massachusetts Institute of Technology under the United States Naval Postgraduate School System through the sponsorship of the Office of Naval Research.

REVENUE

The revenue is derived from the following sources:-
1. The land revenue is levied on all land in the district.
2. The house tax is levied on all houses in the district.
3. The trade tax is levied on all trades in the district.
4. The entertainment tax is levied on all entertainments in the district.
5. The tax on professions, trades and callings is levied on all persons engaged in these occupations.
6. The tax on the sale of liquor is levied on all persons selling liquor.
7. The tax on the sale of opium is levied on all persons selling opium.
8. The tax on the sale of tobacco is levied on all persons selling tobacco.
9. The tax on the sale of betel nuts is levied on all persons selling betel nuts.
10. The tax on the sale of betel leaves is levied on all persons selling betel leaves.

The revenue is paid to the Government of India.
The revenue is used for the following purposes:-
1. For the maintenance of the public works.
2. For the maintenance of the public buildings.
3. For the maintenance of the public institutions.
4. For the maintenance of the public services.
5. For the maintenance of the public order.

TABLE OF CONTENTS

	<u>Page</u>
List of Illustrations	11
List of Tables	111
I. INTRODUCTION	1
II. GENERAL DISCUSSION	4
III. CROSS SECTION	8
IV. COUNTER SENSITIVITY	9
V. NEUTRON YIELD	14
VI. TARGET THICKNESS	22
VII. PROTON ENERGY RESOLUTION	27
VIII. THE CALIBRATED LONG COUNTER	35
IX. THE EXPERIMENT AND RESULTS	42
X. THE APPLICATION OF EQUATION (14)	58
XI. CONCLUSIONS AND RECOMMENDATIONS	60
APPENDIX A: Derivation of G, the fraction of neutrons which enter the counter	62
APPENDIX B: Computations relative to the $\text{Li}^7(\text{p},\text{n})\text{Be}^7$ Reaction	69
APPENDIX C: Possible sequences of certain defined values of the proton energy which occur when integrating over the neutron yield curve	89
BIBLIOGRAPHY	94

TABLE OF CONTENTS

1	1. INTRODUCTION
2	2. SCOPE AND OBJECTIVES
3	3. LITERATURE REVIEW
4	4. METHODOLOGY
5	5. DATA COLLECTION
6	6. DATA ANALYSIS
7	7. RESULTS AND DISCUSSION
8	8. CONCLUSIONS
9	9. REFERENCES
10	10. APPENDICES
11	11. GLOSSARY
12	12. INDEX
13	13. SUMMARY
14	14. ACKNOWLEDGEMENTS
15	15. DECLARATION
16	16. CERTIFICATE
17	17. CURRICULUM VITAE
18	18. STATEMENT OF WORK
19	19. STATEMENT OF ACHIEVEMENT
20	20. STATEMENT OF INTEREST
21	21. STATEMENT OF ACHIEVEMENT
22	22. STATEMENT OF INTEREST
23	23. STATEMENT OF ACHIEVEMENT
24	24. STATEMENT OF INTEREST
25	25. STATEMENT OF ACHIEVEMENT
26	26. STATEMENT OF INTEREST
27	27. STATEMENT OF ACHIEVEMENT
28	28. STATEMENT OF INTEREST
29	29. STATEMENT OF ACHIEVEMENT
30	30. STATEMENT OF INTEREST
31	31. STATEMENT OF ACHIEVEMENT
32	32. STATEMENT OF INTEREST
33	33. STATEMENT OF ACHIEVEMENT
34	34. STATEMENT OF INTEREST
35	35. STATEMENT OF ACHIEVEMENT
36	36. STATEMENT OF INTEREST
37	37. STATEMENT OF ACHIEVEMENT
38	38. STATEMENT OF INTEREST
39	39. STATEMENT OF ACHIEVEMENT
40	40. STATEMENT OF INTEREST
41	41. STATEMENT OF ACHIEVEMENT
42	42. STATEMENT OF INTEREST
43	43. STATEMENT OF ACHIEVEMENT
44	44. STATEMENT OF INTEREST
45	45. STATEMENT OF ACHIEVEMENT
46	46. STATEMENT OF INTEREST
47	47. STATEMENT OF ACHIEVEMENT
48	48. STATEMENT OF INTEREST
49	49. STATEMENT OF ACHIEVEMENT
50	50. STATEMENT OF INTEREST
51	51. STATEMENT OF ACHIEVEMENT
52	52. STATEMENT OF INTEREST
53	53. STATEMENT OF ACHIEVEMENT
54	54. STATEMENT OF INTEREST
55	55. STATEMENT OF ACHIEVEMENT
56	56. STATEMENT OF INTEREST
57	57. STATEMENT OF ACHIEVEMENT
58	58. STATEMENT OF INTEREST
59	59. STATEMENT OF ACHIEVEMENT
60	60. STATEMENT OF INTEREST
61	61. STATEMENT OF ACHIEVEMENT
62	62. STATEMENT OF INTEREST
63	63. STATEMENT OF ACHIEVEMENT
64	64. STATEMENT OF INTEREST
65	65. STATEMENT OF ACHIEVEMENT
66	66. STATEMENT OF INTEREST
67	67. STATEMENT OF ACHIEVEMENT
68	68. STATEMENT OF INTEREST
69	69. STATEMENT OF ACHIEVEMENT
70	70. STATEMENT OF INTEREST
71	71. STATEMENT OF ACHIEVEMENT
72	72. STATEMENT OF INTEREST
73	73. STATEMENT OF ACHIEVEMENT
74	74. STATEMENT OF INTEREST
75	75. STATEMENT OF ACHIEVEMENT
76	76. STATEMENT OF INTEREST
77	77. STATEMENT OF ACHIEVEMENT
78	78. STATEMENT OF INTEREST
79	79. STATEMENT OF ACHIEVEMENT
80	80. STATEMENT OF INTEREST
81	81. STATEMENT OF ACHIEVEMENT
82	82. STATEMENT OF INTEREST
83	83. STATEMENT OF ACHIEVEMENT
84	84. STATEMENT OF INTEREST
85	85. STATEMENT OF ACHIEVEMENT
86	86. STATEMENT OF INTEREST
87	87. STATEMENT OF ACHIEVEMENT
88	88. STATEMENT OF INTEREST
89	89. STATEMENT OF ACHIEVEMENT
90	90. STATEMENT OF INTEREST
91	91. STATEMENT OF ACHIEVEMENT
92	92. STATEMENT OF INTEREST
93	93. STATEMENT OF ACHIEVEMENT
94	94. STATEMENT OF INTEREST
95	95. STATEMENT OF ACHIEVEMENT
96	96. STATEMENT OF INTEREST
97	97. STATEMENT OF ACHIEVEMENT
98	98. STATEMENT OF INTEREST
99	99. STATEMENT OF ACHIEVEMENT
100	100. STATEMENT OF INTEREST

LIST OF ILLUSTRATIONS

	<u>Page</u>
Figure 1. Target thickness versus proton energy difference between threshold and geometric peak for various effective half-angles of the long counter	25
Figure 2. Theoretical counting rate of a calibrated long counter per unit target thickness at 1960-kev proton energy versus effective half-angle of the counter	41
Figure 3. Neutron yield from the $\text{Li}^7(\text{p},\text{n})\text{Be}^7$ reaction for a 6.44-kev thick target; counter at 39.4 inches from target, on beam axis	50
Figure 4. Neutron yield from the $\text{Li}^7(\text{p},\text{n})\text{Be}^7$ reaction for a 6.44-kev thick target; counter at 18.0 inches from target, on beam axis	51
Figure 5. Neutron yield from the $\text{Li}^7(\text{p},\text{n})\text{Be}^7$ reaction for a 6.44-kev thick target; counter at 11.0 inches from target, on beam axis	52
Figure 6. Neutron yield from the $\text{Li}^7(\text{p},\text{n})\text{Be}^7$ reaction for a 6.44-kev thick target; counter at 7.5 inches from target, on beam axis	53
Figure 7. Effective half-angle of the long counter versus distance from the target	57
Figure 8. Schematic representation of the mechanics of an endoergic reaction just above threshold	62a
Figure 9. E_c versus effective half-angle of the counter	73

LIST OF TABLES

	<u>Page</u>
Table I (A-D) Experimentally determined neutron yield data for a 6.44-kev thick lithium target with the long counter located at distances of 39.4, 18.0, 11.0, and 7.5 inches from the target in succession.	46 - 49
Table II Evaluation of E_c for various effective half-angles of the counter (equations 37 and 43)	72
Table III Evaluation of k (equation 38)	74
Table IV Evaluation of $\frac{L(E_c - E_T)}{k^2 + 1/k^2 - 2}$ (Section VI)	75
Table V Evaluation of K and target thickness ΔE (equation 14)	76, 77
Table VI (A-C) Evaluation of terms included in equation 30	78, 79
Table VII (A-H) Evaluation of equation 30 for various values of target thickness and half-angle of the counter	80-87
Table VIII Theoretical relative counting rates of the long counter per unit target thickness at 1960-kev proton energy for various target thicknesses and various counter positions	88

LIST OF TABLES

Table

Table I (a-b)	Geometrical properties of the system	10.0
Table II	Calculation of β for various values of α	10.1
Table III	Calculation of β for various values of α	10.2
Table IV	Calculation of β for various values of α	10.3
Table V	Calculation of β for various values of α	10.4
Table VI (a-b)	Calculation of β for various values of α	10.5
Table VII	Calculation of β for various values of α	10.6
Table VIII	Calculation of β for various values of α	10.7

I. INTRODUCTION

The $\text{Li}(p,n)$ reaction has long been a source of neutrons for experimental work. In many experiments where it is necessary to know the energy resolution of the neutrons, target thickness is the main factor contributing to this resolution, and it becomes imperative to know the value of target thickness within reasonable limits. In other experiments the neutron energy resolution may be due primarily to other effects, such as energy spread of the incident proton beam or the geometry of the experiment; since the neutron energy has an angular dependence, the finite size of materials (scatterers, absorbers, and so forth) introduces a neutron energy spread. For those experiments that fall in the latter category, as is probable when using very thin targets, an accurate determination of target thickness is not important from the viewpoint of determining the neutron energy resolution. However, even here, other considerations may require that target thickness be accurately determined.

There are many articles in the literature dealing with endo-ergic reactions in general and the $\text{Li}(p,n)$ reaction in particular, noteworthy among which is the work of Hansen, Taschek, and Williams¹. As a result of their work, they observed that by using a conventional 8-inch long counter for neutron detection, located 1 meter from the target along the beam axis, the difference between the proton energy at the geometric peak and at threshold was a good approximation of target thickness. This method of determining target thickness is

commonly used and is referred to as the "rise" method. They also discussed the use of a calibrated counter for determining the thickness of fresh lithium targets.

In the course of certain experiments at this Laboratory, a question arose concerning the accuracy of the rise method of determining target thickness, and, further, the effect of moving the counter closer to the target in order to obtain higher counting rates. This thesis is the result of a study to answer the above questions. During the course of this work, it was found that target thickness had been determined previously^{2,3} in at least two cases by fitting a theoretical yield curve to the experimental curve, but no thorough treatment of this method has been found. Such a method should give accurate results if the energy spread of the incident beam and straggling within the target are considered.

It would seem, however, that this method must be tedious, since two parameters, target thickness and effective half-angle of the counter, must be adjusted by trial and error until a best fit is obtained over the rise portion of the geometric peak. Whereas the shape of the rise portion of the curve and the height of the peak depend rather strongly on the proton energy spread within the target, the proton energy at which the peak occurs is not strongly dependent on the proton energy resolution. This situation is quite similar to the effect of resolution on the shape of a cross-section resonance.

1. The first step is to identify the problem or question that needs to be answered. This involves understanding the context and the specific requirements of the task.

[illegible][illegible]

It is because of this that the rise method can be used for determining the target thickness in the manner indicated in this thesis.

The total number of particles from a thin target of thickness t , assuming an incident beam of monoenergetic particles with an energy E and the number of particles in the target, N , is

$$(1) \quad N_{\text{total}} = N \sigma \int_0^t \frac{1}{x} dx = N \sigma \ln \frac{t}{x_0}$$

where x_0 is the initial thickness of the target, σ is the cross-section of the target, and N is the number of particles in the target.

Let E_0 = energy of particles incident upon the target

E = energy of particles after the target

$E_0 - E$ = energy dissipated

$\phi(E)$ = cross-section for the reaction

$\phi(E)$ = function of energy from classical mechanics of particles, which varies with energy.

Then it can be written

$$(2) \quad N_{\text{total}} = N \sigma \int_0^t \frac{1}{x} dx = N \sigma \ln \frac{t}{x_0}$$

where t is the thickness of the target, x_0 is the initial thickness of the target, σ is the cross-section of the target, and N is the number of particles in the target.

where t is the thickness of the target, x_0 is the initial thickness of the target, σ is the cross-section of the target, and N is the number of particles in the target.

Assuming that the particles are incident on the target from the left, the number of particles in the target is

be represented as in Figure 8, Appendix A. The reaction is pictured as occurring at the center of sphere A, the radius (V_n) representing the velocity of the neutron in the center-of-mass system. To transform to the laboratory system, it is only necessary to add the velocity of the center of mass to each point on the surface of sphere A, thus obtaining sphere B, also of radius V_n . A vector from the center of sphere A to any point on the surface of sphere B represents a particular neutron velocity (energy) in the laboratory. Thus, a group of neutrons appears in the laboratory with essentially a continuum of velocities ranging from a minimum value ($V_{cm} - V_n$) to a maximum value ($V_{cm} + V_n$), both occurring at zero degrees.

At threshold the neutrons are "squeezed" out of the nucleus with velocity (V_n) equal to zero. In this limiting case, spheres A and B are reduced to points, and all of the neutrons appear at zero degrees in the laboratory with a velocity equal to that of the center of mass. At a slightly higher proton energy, spheres A and B have a finite size as depicted in Figure 8. Here, sphere B defines a cone of neutrons of half-angle γ . At any angle less than γ , sphere B is intercepted in two points corresponding to two different neutron energies. Consequently, an element of solid angle within the neutron cone will intercept two groups of neutrons of different energies.

Since the neutron cone is defined by the angle γ for which the cone and sphere are tangent, it follows that the point of tangency corresponds to neutrons of a particular energy.

[illegible]

The cone gets larger with increasing proton energy until the neutron velocity in the center-of-mass system is equal to the center-of-mass velocity, at which time the cone has opened up to 2π steradians so that neutrons are being emitted into the entire forward hemisphere in the laboratory. The proton energy at which this occurs is designated E_L , and at this energy the lower-energy neutron group disappears. With any further increase of proton energy above E_L , neutrons are emitted throughout the entire 4π steradians of the laboratory.

With the long counter placed with its axis along the beam axis, the fraction (G) of neutrons emitted from thickness dE which enters the counter depends on the size of the neutron cone and the half-angle (θ) which the counter subtends at the target. If E_c is defined as that proton energy at which the neutron cone is equal to the cone subtended by the counter, then the fraction (G) has the following values (Appendix A):

$$(3a) \quad G_1 = 1 \quad . \quad . \quad . \quad . \quad . \quad . \quad . \quad . \quad . \quad . \quad E < E_c$$

$$(3b) \quad G_2 = 1 - k \left(\frac{E - E_c}{E - E_T} \right)^{1/2} \quad . \quad . \quad . \quad . \quad . \quad . \quad E_c < E < E_L$$

$$(3c) \quad G_3 = 1/2 \left[1 - k \left(\frac{E - E_c}{E - E_T} \right)^{1/2} + b \left(\frac{E}{E - E_T} \right)^{1/2} \right] \quad . \quad E > E_L$$

where

$$k = \left(1 - \frac{m_1 m_3}{m_2 m_4} \sin^2 \theta \right)^{1/2} \cos \theta = \left(\frac{E_T}{E_c} \right)^{1/2} \cos \theta$$

$$b = \left(\frac{m_1 m_3}{m_2 m_4} \right)^{1/2} \sin^2 \theta$$

The new data suggest a different picture of the
 behavior of the system at high values of the
 parameter λ . It is clear that the system is
 in a state of oscillation for all values of λ .
 In the limit $\lambda \rightarrow \infty$, the system tends to a
 state of oscillation with a period of 2π .
 This is in agreement with the results of the
 numerical calculations.

With the help of the results of the
 numerical calculations, we can show that
 the system is in a state of oscillation
 for all values of λ . In fact, we can
 show that the system is in a state of
 oscillation for all values of λ . This
 is in agreement with the results of the
 numerical calculations.

$$(1) \quad \lambda > 1 \quad \dots \quad \lambda > 1$$

$$(2) \quad \lambda > 1 \quad \dots \quad \lambda > 1$$

$$(3) \quad \lambda < 1 \quad \dots \quad \lambda < 1$$

$$\lambda = 1 \quad \dots \quad \lambda = 1$$

and $m_{1,2,3,4}$ are the masses of the projectile particle, target nucleus, resultant particle, and product nucleus, respectively.

III. CROSS SECTION

From theoretical considerations, it is shown⁴ that, for a neutron emitted with angular momentum ℓ , the cross section at energies just above threshold is given by:

$$(4) \quad \sigma_{\ell}(a,n) = \text{const } E_n^{\ell + 1/2}$$

where "a" is the charged particle inducing the reaction, and E_n is the neutron energy in the center-of-mass system. Because of the high centrifugal barrier in the region just above threshold for neutrons with angular momentum other than zero⁵, the contribution to the yield from such neutrons will be small compared with that from neutrons having zero angular momentum, hence no centrifugal barrier.

Since the threshold neutrons mostly have $\ell = 0$,

$$(5) \quad \sigma(a,n) = \text{const } E_n^{1/2} = \text{const } V_n.$$

In Appendix A, it is shown that the neutron velocity in the center-of-mass system is given by:

$$V_n = \text{const } (E - E_T)^{1/2}$$

where E_T is the threshold energy and E the instantaneous energy of the incident particle. Then the cross section σ may be written:

$$(6) \quad \sigma = C(E - E_T)^{1/2} \quad \text{where } C \text{ is a constant.}$$

IV. COUNTER SENSITIVITY

The 8-inch long counter⁶ is the result of several attempts to find an arrangement of paraffin surrounding a boron detector such that the number of boron disintegrations is proportional to the number of primary-source neutrons and independent of their energies over a wide range. This counter consists of a paraffin cylinder 12 inches in length and 8 inches in diameter. Along its axis is a BF_3 proportional counter 1 inch in diameter and 8 inches in active length is embedded. It protrudes slightly over the front face of the paraffin but is protected from direct thermal neutrons by a cadmium shield. An aluminum tube shields the counter electrically. For insulation, the space between the counter wall and the shield is filled with ceresin wax. The central electrode consists of a Kovar wire of 10-mil diameter. The counter is filled with enriched (80 percent B^{10}) BF_3 to a pressure of 25 cm Hg. With 2700 volts applied to the wall a gas multiplication of about 10 is obtained. With the source of neutrons placed on the counter axis one meter from the face, a flat response is obtained in the region from about 0.5 to 3.0 Mev. The performance of the counter may be explained qualitatively as follows.

The length of the counter is many times greater than the mean free path of any neutrons to be detected. Neutrons entering the paraffin are degraded to thermal energies and diffuse into the detector where they give rise to $\text{B}(n,\alpha)$ reactions. Because of the large

cross section, the counting rate is determined essentially by the flux of thermal neutrons. For an infinitely large slab of paraffin, the efficiency would increase with increasing neutron energy, since low-energy neutrons penetrate only a short distance into the paraffin before being thermalized. Therefore, the low-energy neutrons have a better chance of escaping through the front face (instead of passing through the detector) than neutrons that were originally of higher energy and are thermalized at a greater distance from the front face. There are two reasons for this. At higher energies, more collisions are required for thermalization, and the collision cross section is smaller than at low energies. In order to minimize the dependence of the efficiency on the energy, the dimensions of the paraffin must be such that the thermalized fast neutrons have an increased chance to escape from the paraffin.

The probability that a neutron striking a long counter will be counted is a function of its energy and direction, and the distance from the counter axis at which it strikes. The conventional 8-inch long counter has been designed to give a flat response in the region from about 0.5 to 3 Mev, for a uniform distribution over the face of the counter. The situation is somewhat different in this problem as the neutrons are emitted in a cone of varying solid angle within which the energy distribution is not uniform. Only after the cone has opened up to 4π steradians is the distribution approximately uniform over the counter face, but the forward direction is still favored.

When working the working rule is followed consistently by the
 that of the first position. The is relatively large and of working,
 the attachment with the same with the same, then
 the working position consists only a short distance into the working
 before being finished. However, the working position has a
 better sense of working than the first (based on working
 through the device) than working that way slightly at right

energy and are themselves at a greater distance from the first line.
 There are two reasons for this. In higher position, one position
 are required for the working, and the working cross section is
 smaller than at the working. In order to obtain the optimum
 of the efficiency in the working, the distance of the working

must be such that the working and working are in the same
 position as when the working.

The working rule is a working position a long working rule
 be working in a position of the working and working, and the dis-
 tance from the working rule is small in working. The working
 position is working and working in the same position in the
 position from the rule in a way, the working position was the
 same of the working. The working is working in the

position in the working are added in a way of working with the
 working with the working in working in the working. The working
 rule the working is in the working in the working position.
 working rule the working rule, the working position is 1000

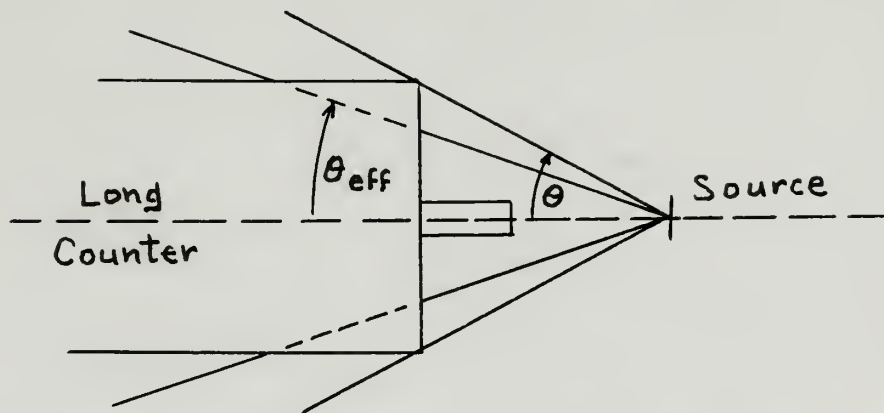
A theoretical calculation of counter sensitivity would be very difficult, if not impossible. It seems that the best solution to the problem is to consider counter sensitivity as being constant, and to use a counter which is modified to best satisfy this assumption consistent with reasonable yield.

For proton energies up to 40 kev above threshold, neutron energies will range from a few kev to about 120 kev. (Figure 13 of reference 1.) For each proton energy in this range, the counter will intercept all of the neutrons if $E < E_c$ or two groups, high and low energy, if $E > E_c$. Because of the finite thickness of the target, both situations can occur simultaneously. The net result is that neutrons of various energies are incident upon the counter for any proton energy.

The experimental sensitivity curves of Hanson and McKibben⁶ show that a 6-inch paraffin diameter gives a flatter response than the conventional 8-inch counter for neutrons in the energy range from thermal to a few hundred kev. This is explained by the fact that the sensitivity of the counter to high-energy neutrons is decreased because of the smaller mass of paraffin, and the sensitivity to low-energy neutrons is therefore relatively high. It may be inferred that a paraffin diameter less than 6 inches will give a still flatter response over the energy range of interest. Snowden and Whitehead² have used a 4-inch paraffin diameter in their work of fitting a theoretical yield curve to the experimental yield curve.

R. A. Nobles et al⁷ have modified the shielded long counter⁶ by employing a BF_3 counter of larger diameter placed slightly farther forward in the paraffin moderator. Whereas the conventional shielded long counter shows a 10 percent drop in efficiency at 25 kev compared to the flat response region, it is claimed for the modified counter that no decrease in efficiency has occurred at 25 kev.

In the design of the optimum counter, another factor must be considered. Those neutrons which strike near the outer periphery of the paraffin have a velocity which is at an angle with respect to the counter axis. This may be represented as follows:



These neutrons have a higher probability of escaping from the counter because of the smaller amount of paraffin in the direction of their motion. The result is that the counter will have an effective half-angle (θ_{eff}) less than its true half-angle (θ). This effect is increased as the counter is moved closer to the target. It seems that

the use of a truncated cone of paraffin as employed by Bonner and Butler³ would reduce this effect. However, for optimum results, this would demand a separate truncated cone for each position of the counter. Even then, one could not expect the loss of counts to occur sharply at $E = E_c$. Possibly the best practical counter would be one having a truncated cone corresponding to the average position at which the counter is expected to be used.

The benefits of such an optimum design may not be sufficient to offset the advantage of using the conventional counter. In either case, it will be necessary to know the effective half-angle of the counter for various counter positions.

V. NEUTRON YIELD

Letting $\epsilon = \text{constant}$ and $\sigma = C(E - E_T)^{1/2}$ in accordance with the foregoing discussions, equation (2) becomes:

$$(7) \quad N_C = Z \int_{E_0 - \Delta E}^{E_0} G (E - E_T)^{1/2} dE$$

where $Z = N n f \epsilon C = \text{a constant}$, and $\Delta E = \text{target thickness}$.

Equations (3a,b,c) indicate that the form of the analytical expression defining G depends on the value of E at the point in question. This causes the integral of equation (7) to break up into two integrals if at any point within the target the proton energy has the value E_C or E_L . In order to evaluate equation (7) over the yield curve from threshold to a point beyond the geometric peak, it is necessary to know the sequence of E values. Only then can the proper G value and the limits of integration be correctly selected. Of the five possible sequences of E values discussed in Appendix B, it is there shown that only the following two sequences can occur for counter half-angles less than 30 degrees and target thicknesses less than 30 kev. (These two sequences are arranged in order of increasing E and will hereafter be referred to as cases I and II):

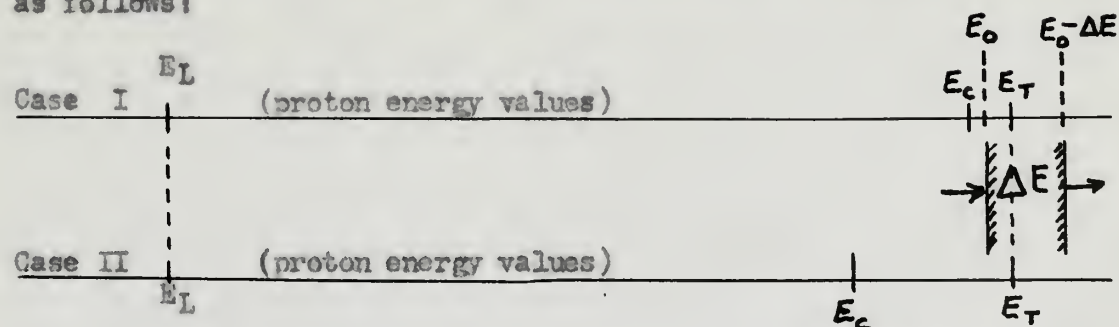
<u>I</u>	<u>II</u>
E_T	E_T
E_O	$E_T + \Delta E$
$E_T + \Delta E$	E_C
$E_C + \Delta E$	$E_C + \Delta E$
E_L	E_L
$E_L + \Delta E$	$E_L + \Delta E$

For target thicknesses up to $(E_L - E_T)/2$ (19.85 kev for lithium), case I will occur for $E_C < (E_T + \Delta E)$ and case II for $E_C > (E_T + \Delta E)$. Only case I can occur for

$$\left(\frac{E_L - E_T}{2} \right) < \Delta E < (E_L - E_C)$$

which for lithium is: 19.85 kev $< \Delta E < 30$ kev.

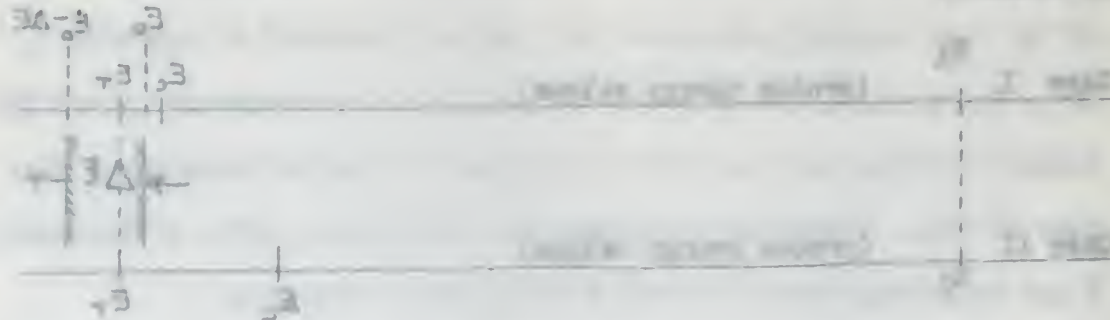
These two sequences may be illustrated in a typical situation as follows:



As the proton energy scales move to the right relative to the target of thickness ΔE , they indicate the manner in which the various

For the first inequality we use $(\mathcal{H}_1^2)^2 = \mathcal{H}_1^4$ and $\mathcal{H}_1^2 \leq \mathcal{H}_1^4$ and obtain $\mathcal{H}_1^2 \leq \mathcal{H}_1^4$ and $\mathcal{H}_1^2 \leq \mathcal{H}_1^4$.

There are two important properties of the function f :



increased the number of women who completed the study, the percentage of women who dropped out of the study was 10.5%.

Suppose that the following conditions are satisfied:

(i) $\lim_{n \rightarrow \infty} \frac{1}{n} \sum_{k=1}^n \frac{1}{k} = 0$

$$(1) \quad \lim_{n \rightarrow \infty} \frac{1}{n} \sum_{k=1}^n \frac{1}{k} = 0$$

$$(2) \quad \lim_{n \rightarrow \infty} \frac{1}{n} \sum_{k=1}^n \frac{1}{k^2} = 0$$

$$(3) \quad \lim_{n \rightarrow \infty} \frac{1}{n} \sum_{k=1}^n \frac{1}{k^3} = 0$$

$$(4) \quad \lim_{n \rightarrow \infty} \frac{1}{n} \sum_{k=1}^n \frac{1}{k^4} = 0$$

$$(5) \quad \lim_{n \rightarrow \infty} \frac{1}{n} \sum_{k=1}^n \frac{1}{k^5} = 0$$

$$(6) \quad \lim_{n \rightarrow \infty} \frac{1}{n} \sum_{k=1}^n \frac{1}{k^6} = 0$$

Case II: Nc/Z equals

$$(9a) \int_{E_T}^{E_0} G_1 \sigma \, dE \quad . \quad . \quad . \quad . \quad . \quad . \quad . \quad E_T < E_0 < E_T + \Delta E$$

$$(9b) \int_{E_0 - \Delta E}^{E_0} G_1 \sigma \, dE \quad . \quad . \quad . \quad . \quad . \quad . \quad . \quad E_T + \Delta E < E_0 < E_C$$

$$(9c) \int_{E_0 - \Delta E}^{E_C} G_1 \sigma \, dE + \int_{E_C}^{E_0} G_2 \sigma \, dE \quad . \quad . \quad . \quad E_C < E_0 < E_C + \Delta E$$

(9d,e,f) These are identical to (8d,e,f), respectively.

It is seen from equations (3a,b,c) that $G \sigma$ has the values:

$$G_1 \sigma = (E - E_T)^{1/2}$$

$$G_2 \sigma = (E - E_T)^{1/2} - k(E - E_C)^{1/2} = G_1 \sigma - k(E - E_C)^{1/2}$$

$$G_3 \sigma = 1/2 (E - E_T)^{1/2} - k(E - E_C)^{1/2} + b E^{1/2}$$

$$= 1/2 G_2 \sigma + b E^{1/2}$$

Substituting these expressions for $G_{1,2,3} \sigma$ in equations (8) and (9) gives:

Case I: Nc/Z equals

$$(10a) \int_{E_T}^{E_0} (E - E_T)^{1/2} dE \quad . \quad . \quad . \quad . \quad . \quad . \quad E_T < E_0 < E_C$$

$$(10b) \int_{E_T}^{E_0} (E - E_T)^{1/2} dE - k \int_{E_C}^{E_0} (E - E_C)^{1/2} dE \quad . \quad E_C < E_0 < E_T + \Delta E$$

$$(10c) \int_{E_0 - \Delta E}^{E_0} (E - E_T)^{1/2} dE - k \int_{E_C}^{E_0} (E - E_C)^{1/2} dE \quad . \quad E_T + \Delta E < E_0 < E_C + \Delta E$$

$$(10d) \int_{E_0 - \Delta E}^{E_0} \left[(E - E_T)^{1/2} - k(E - E_C)^{1/2} \right] dE \quad . \quad . \quad . \quad . \quad E_C + \Delta E < E_0 < E_L$$

$$(10e) \int_{E_0 - \Delta E}^{E_0} \left[(E - E_T)^{1/2} - k(E - E_C)^{1/2} \right] dE - 1/2 \int_{E_L}^{E_0} \left[(E - E_T)^{1/2} \right.$$

$$\left. - k(E - E_C)^{1/2} - b E^{1/2} \right] dE \quad . \quad . \quad . \quad E_L < E_0 < E_L + \Delta E$$

$$(10f) 1/2 \int_{E_0 - \Delta E}^{E_0} \left[(E - E_T)^{1/2} - k(E - E_C)^{1/2} + b E^{1/2} \right] dE \quad E_0 > E_L + \Delta E$$

Case II: Nc/Z equals

$$(11a) \int_{E_T}^{E_0} (E - E_T)^{1/2} dE \quad . \quad . \quad . \quad . \quad . \quad . \quad E_T < E_0 < E_T + \Delta E$$

$$(11b) \int_{E_0 - \Delta E}^{E_0} (E - E_T)^{1/2} dE \quad . \quad . \quad . \quad . \quad . \quad . \quad E_T + \Delta E < E_0 < E_C$$

$$(11c) \int_{E_0 - \Delta E}^{E_0} (E - E_T)^{1/2} dE - k \int_{E_C}^{E_0} (E - E_C)^{1/2} dE \quad . \quad E_C < E_0 < E_C + \Delta E$$

(11d,e,f) These are identical to (10d,e,f), respectively.

Integration of equations (10) and (11) give the following expressions:

1990 1991 1992 1993 1994 1995 1996 1997 1998 1999 2000 2001 2002 2003 2004 2005 2006 2007 2008 2009 2010 2011 2012 2013 2014 2015 2016 2017 2018 2019 2020 2021 2022 2023 2024 2025 2026 2027 2028 2029 2030 2031 2032 2033 2034 2035 2036 2037 2038 2039 2040 2041 2042 2043 2044 2045 2046 2047 2048 2049 2050 2051 2052 2053 2054 2055 2056 2057 2058 2059 2060 2061 2062 2063 2064 2065 2066 2067 2068 2069 2070 2071 2072 2073 2074 2075 2076 2077 2078 2079 2080 2081 2082 2083 2084 2085 2086 2087 2088 2089 2090 2091 2092 2093 2094 2095 2096 2097 2098 2099 2100 2101 2102 2103 2104 2105 2106 2107 2108 2109 2110 2111 2112 2113 2114 2115 2116 2117 2118 2119 2120 2121 2122 2123 2124 2125 2126 2127 2128 2129 2130 2131 2132 2133 2134 2135 2136 2137 2138 2139 2140 2141 2142 2143 2144 2145 2146 2147 2148 2149 2150 2151 2152 2153 2154 2155 2156 2157 2158 2159 2160 2161 2162 2163 2164 2165 2166 2167 2168 2169 2170 2171 2172 2173 2174 2175 2176 2177 2178 2179 2180 2181 2182 2183 2184 2185 2186 2187 2188 2189 2190 2191 2192 2193 2194 2195 2196 2197 2198 2199 2200 2201 2202 2203 2204 2205 2206 2207 2208 2209 2210 2211 2212 2213 2214 2215 2216 2217 2218 2219 2220 2221 2222 2223 2224 2225 2226 2227 2228 2229 2230 2231 2232 2233 2234 2235 2236 2237 2238 2239 2240 2241 2242 2243 2244 2245 2246 2247 2248 2249 2250 2251 2252 2253 2254 2255 2256 2257 2258 2259 2260 2261 2262 2263 2264 2265 2266 2267 2268 2269 2270 2271 2272 2273 2274 2275 2276 2277 2278 2279 2280 2281 2282 2283 2284 2285 2286 2287 2288 2289 2290 2291 2292 2293 2294 2295 2296 2297 2298 2299 2300 2301 2302 2303 2304 2305 2306 2307 2308 2309 2310 2311 2312 2313 2314 2315 2316 2317 2318 2319 2320 2321 2322 2323 2324 2325 2326 2327 2328 2329 2330 2331 2332 2333 2334 2335 2336 2337 2338 2339 2340 2341 2342 2343 2344 2345 2346 2347 2348 2349 2350 2351 2352 2353 2354 2355 2356 2357 2358 2359 2360 2361 2362 2363 2364 2365 2366 2367 2368 2369 2370 2371 2372 2373 2374 2375 2376 2377 2378 2379 2380 2381 2382 2383 2384 2385 2386 2387 2388 2389 2390 2391 2392 2393 2394 2395 2396 2397 2398 2399 2400 2401 2402 2403 2404 2405 2406 2407 2408 2409 2410 2411 2412 2413 2414 2415 2416 2417 2418 2419 2420 2421 2422 2423 2424 2425 2426 2427 2428 2429 2430 2431 2432 2433 2434 2435 2436 2437 2438 2439 2440 2441 2442 2443 2444 2445 2446 2447 2448 2449 2450 2451 2452 2453 2454 2455 2456 2457 2458 2459 2460 2461 2462 2463 2464 2465 2466 2467 2468 2469 2470 2471 2472 2473 2474 2475 2476 2477 2478 2479 2480 2481 2482 2483 2484 2485 2486 2487 2488 2489 2490 2491 2492 2493 2494 2495 2496 2497 2498 2499 2500 2501 2502 2503 2504 2505 2506 2507 2508 2509 2510 2511 2512 2513 2514 2515 2516 2517 2518 2519 2520 2521 2522 2523 2524 2525 2526 2527 2528 2529 2530 2531 2532 2533 2534 2535 2536 2537 2538 2539 2540 2541 2542 2543 2544 2545 2546 2547 2548 2549 2550 2551 2552 2553 2554 2555 2556 2557 2558 2559 2560 2561 2562 2563 2564 2565 2566 2567 2568 2569 2570 2571 2572 2573 2574 2575 2576 2577 2578 2579 2580 2581 2582 2583 2584 2585 2586 2587 2588 2589 2590 2591 2592 2593 2594 2595 2596 2597 2598 2599 2600 2601 2602 2603 2604 2605 2606 2607 2608 2609 2610 2611 2612 2613 2614 2615 2616 2617 2618 2619 2620 2621 2622 2623 2624 2625 2626 2627 2628 2629 2630 2631 2632 2633 2634 2635 2636 2637 2638 2639 2640 2641 2642 2643 2644 2645 2646 2647 2648 2649 2650 2651 2652 2653 2654 2655 2656 2657 2658 2659 2660 2661 2662 2663 2664 2665 2666 2667 2668 2669 2670 2671 2672 2673 2674 2675 2676 2677 2678 2679 2680 2681 2682 2683 2684 2685 2686 2687 2688 2689 2690 2691 2692 2693 2694 2695 2696 2697 2698 2699 2700 2701 2702 2703 2704 2705 2706 2707 2708 2709 2710 2711 2712 2713 2714 2715 2716 2717 2718 2719 2720 2721 2722 2723 2724 2725 2726 2727 2728 2729 2730 2731 2732 2733 2734 2735 2736 2737 2738 2739 2740 2741 2742 2743 2744 2745 2746 2747 2748 2749 2750 2751 2752 2753 2754 2755 2756 2757 2758 2759 2760 2761 2762 2763 2764 2765 2766 2767 2768 2769 2770 2771 2772 2773 2774 2775 2776 2777 2778 2779 2780 2781 2782 2783 2784 2785 2786 2787 2788 2789 2790 2791 2792 2793 2794 2795 2796 2797 2798 2799 2800 2801 2802 2803 2804 2805 2806 2807 2808

$$\log p_1 \geq \log p_2 \geq \log p_3 \geq \dots \geq \log p_n \geq \log p_{n+1} = 0 \quad \text{with} \quad \sum_{i=1}^n p_i = 1 \quad \text{and} \quad \sum_{i=1}^n p_i \log p_i = -H(X)$$

$$\mu^2 > \mu^2 > \mu^2 + \mu^2 \dots \dots \dots \mu^2_{(1/2)} (1/2) \dots \dots \dots \mu^2_{(1/2)} (1/2)$$

$$\exp(\beta) \geq \exp(\beta) \cdot \exp\left(\frac{1}{2}(\beta - \beta)\right) = \exp(\beta) \cdot \exp\left(\frac{1}{2}(\beta - \beta)\right) = \exp(\beta)$$

gibt es ein $\delta \in (0, 1)$ mit $\delta \leq \delta_0$ und $\delta \leq \delta_1$ so dass

Information on weights (20) and (21) is the following

Case I: $3N_c/2Z$ equals

$$(12a) \quad (E_0 - E_T)^{3/2} \dots \dots \dots E_T < E_0 < E_c$$

$$(12b) \quad (E_0 - E_T)^{3/2} - k(E_0 - E_c)^{3/2} \dots \dots \dots E_c < E_0 < E_T + \Delta E$$

$$(12c) \quad (E_0 - E_T)^{3/2} - (E_0 - E_T - \Delta E)^{3/2} - k(E_0 - E_c)^{3/2} \dots E_T + \Delta E < E_0 < E_c + \Delta E$$

$$(12d) \quad (E_0 - E_T)^{3/2} - (E_0 - E_T - \Delta E)^{3/2} - k \left[(E_0 - E_c)^{3/2} - (E_0 - E_c - \Delta E)^{3/2} \right] \dots \dots \dots E_c + \Delta E < E_0 < E_L$$

$$(12e) \quad 1/2 \left\{ (E_0 - E_T)^{3/2} - 2(E_0 - E_T - \Delta E)^{3/2} + (E_L - E_T)^{3/2} + b(E_0^{3/2} - E_L^{3/2}) \right. \\ \left. - k \left[(E_0 - E_c)^{3/2} - 2(E_0 - E_c - \Delta E)^{3/2} + (E_L - E_c)^{3/2} \right] \right\} E_L < E_0 < E_L + \Delta E$$

$$(12f) \quad 1/2 \left\{ (E_0 - E_T)^{3/2} - (E_0 - E_T - \Delta E)^{3/2} + b \left[E_0^{3/2} - (E_0 - \Delta E)^{3/2} \right] \right. \\ \left. - k \left[(E_0 - E_c)^{3/2} - (E_0 - E_c - \Delta E)^{3/2} \right] \right\} \dots \dots \dots E_0 > E_L + \Delta E$$

Case II: $3N_c/2Z$ equals

$$(13a) \quad (E_0 - E_T)^{3/2} \dots \dots \dots E_T < E_0 < E + \Delta E$$

$$(13b) \quad (E_0 - E_T)^{3/2} - (E_0 - E_T - \Delta E)^{3/2} \dots \dots \dots E_T + \Delta E < E_0 < E_c$$

$$(13c) \quad (E_0 - E_T)^{3/2} - (E_0 - E_T - \Delta E)^{3/2} - k(E_0 - E_c)^{3/2} \dots E_c < E_0 < E_c + \Delta E$$

(13d,e,f) These are identical to (12d,e,f), respectively.

where $\mathcal{P}_1, \mathcal{P}_2, \dots, \mathcal{P}_n$ are

$$\mathcal{P}_1 > \mathcal{P}_2 > \mathcal{P}_3 > \dots > \mathcal{P}_n \quad (121)$$

$$\mathcal{P}_1 > \mathcal{P}_2 > \mathcal{P}_3 > \dots > \mathcal{P}_n \quad (122)$$

$$\mathcal{P}_1 > \mathcal{P}_2 > \mathcal{P}_3 > \dots > \mathcal{P}_n \quad (123)$$

$$[\mathcal{P}_1(\mathcal{P}_2 - \mathcal{P}_3 - \mathcal{P}_4) - \mathcal{P}_2(\mathcal{P}_3 - \mathcal{P}_4)] > \mathcal{P}_3(\mathcal{P}_4 - \mathcal{P}_5) - \mathcal{P}_4(\mathcal{P}_5 - \mathcal{P}_6) \quad (124)$$

$$\mathcal{P}_1 > \mathcal{P}_2 > \mathcal{P}_3 > \dots > \mathcal{P}_n$$

$$\{\mathcal{P}_1(\mathcal{P}_2 - \mathcal{P}_3) + \mathcal{P}_2(\mathcal{P}_3 - \mathcal{P}_4) + \mathcal{P}_3(\mathcal{P}_4 - \mathcal{P}_5) + \dots + \mathcal{P}_n(\mathcal{P}_n - \mathcal{P}_1)\} > 0 \quad (125)$$

$$\mathcal{P}_1 > \mathcal{P}_2 > \mathcal{P}_3 > \dots > \mathcal{P}_n \quad \left\{ \mathcal{P}_1(\mathcal{P}_2 - \mathcal{P}_3) + \mathcal{P}_2(\mathcal{P}_3 - \mathcal{P}_4) + \mathcal{P}_3(\mathcal{P}_4 - \mathcal{P}_5) + \dots + \mathcal{P}_n(\mathcal{P}_n - \mathcal{P}_1) \right\} > 0$$

$$\left\{ \mathcal{P}_1(\mathcal{P}_2 - \mathcal{P}_3) + \mathcal{P}_2(\mathcal{P}_3 - \mathcal{P}_4) + \mathcal{P}_3(\mathcal{P}_4 - \mathcal{P}_5) + \dots + \mathcal{P}_n(\mathcal{P}_n - \mathcal{P}_1) \right\} > 0 \quad (126)$$

$$\mathcal{P}_1 > \mathcal{P}_2 > \mathcal{P}_3 > \dots > \mathcal{P}_n \quad \left\{ \mathcal{P}_1(\mathcal{P}_2 - \mathcal{P}_3) + \mathcal{P}_2(\mathcal{P}_3 - \mathcal{P}_4) + \mathcal{P}_3(\mathcal{P}_4 - \mathcal{P}_5) + \dots + \mathcal{P}_n(\mathcal{P}_n - \mathcal{P}_1) \right\} > 0$$

where $\mathcal{P}_1, \mathcal{P}_2, \dots, \mathcal{P}_n$ are

$$\mathcal{P}_1 > \mathcal{P}_2 > \mathcal{P}_3 > \dots > \mathcal{P}_n \quad (127)$$

$$\mathcal{P}_1 > \mathcal{P}_2 > \mathcal{P}_3 > \dots > \mathcal{P}_n \quad (128)$$

$$\mathcal{P}_1 > \mathcal{P}_2 > \mathcal{P}_3 > \dots > \mathcal{P}_n \quad (129)$$

(121)-(129) are the same as (121)-(129) in [12].

These equations may be used for computing a theoretical yield curve. A word of caution must be injected at this point concerning equations (12e,f) and (13e,f). These have been derived from the assumption that $\sigma = C(E - E_T)^{1/2}$, and they will prove useful for reactions where that assumption is valid for the regions in question. The cross section for the $\text{Li}(p,n)$ reaction, however, is almost constant throughout portions of the regions to which these equations apply. This is no handicap, however, since the equations (12a-d) and (13a-d) enable one to compute a theoretical yield curve for target thicknesses up to 30 kev which is the limit of thickness being considered.

These conditions are to be used for computing a theoretical yield curve. A curve of constant yield is plotted as a line connecting the points (10, 10) and (100, 10). These have been derived from the assumption that $r = 0.05$ and they will have useful for purposes where that assumption is valid for the purpose in question. The curve for the 10% yield, however, is almost everywhere throughout the range of the yield in which these equations apply. This is as indicated, however, above the equation (10-1) and (10-2) points are to compute a theoretical yield curve for the 10% yield as to the yield of the 10% of the 10% yield.

continued.

VI. TARGET THICKNESS

A visual inspection of equations (12a,b) and (13a,b) shows that the geometric peak must occur for:

$$\text{Case I: } E_0 > E_T + \Delta E$$

$$\text{Case II: } E_0 > E_C$$

The requirement that the peak occur in the region defined by equations (12c) and (13c) for Cases I and II, respectively, is in either case:

$$N_G(\text{at } E_0 = E_C + \Delta E - \epsilon) > N_G(\text{at } E_0 = E_C + \Delta E)$$

where ϵ is an infinitesimal.

Utilizing equation (12c) or (13c), the requirement is:

$$(E_C - E_T + \Delta E - \epsilon)^{3/2} - (E_C - E_T - \epsilon)^{3/2} - k(\Delta E - \epsilon)^{3/2} >$$

$$(E_C - E_T + \Delta E)^{3/2} - (E_C - E_T)^{3/2} - k(\Delta E)^{3/2}$$

Expanding and collecting terms:

$$3/2 \quad \epsilon \left[(E_C - E_T)^{1/2} - (E_C - E_T + \Delta E)^{1/2} + k(\Delta E)^{1/2} \right] > 0$$

$$(E_C - E_T)^{1/2} + k(\Delta E)^{1/2} > (E_C - E_T + \Delta E)^{1/2}$$

Squaring both sides:

$$k^2 \Delta E + 2k(\Delta E)^{1/2}(E_c - E_T)^{1/2} > \Delta E$$

$$\left(\frac{1 - k^2}{2k}\right)^2 \Delta E < E_c - E_T$$

$$\Delta E < \frac{4(E_c - E_T)}{k^2 + 1/k^2 - 2}$$

Evaluation of the expression on the right-hand side of this inequality (Table IX, Appendix B) for values of θ between zero and 30 degrees, shows that this inequality holds for target thicknesses up to about 400 kev. Thus, the peak will occur in the regions defined by equations (12c) and (13c) for Cases I and II, respectively. Taking the derivative of N_c with respect to E_0 in this region and evaluating at the peak position:

$$\left. \frac{dN_c}{dE_0} \right|_{E_p} = 0, \text{ where } E_p \text{ is the incident particle energy at the}$$

peak position.

$$(14) \quad \Delta E = E_p - E_T - K$$

$$\begin{aligned} \text{where } K &= \left[(E_p - E_T)^{1/2} - k(E_p - E_c)^{1/2} \right]^2 \\ &= \left[(E_p - E_T)^{1/2} - \cos \theta \cdot E_T^{1/2} \left(\frac{E_D}{E_c} - 1 \right)^{1/2} \right]^2 \end{aligned}$$

The correction term (K) and the target thickness (ΔE) are evaluated in Table X for various values of the effective half-angle of the counter (θ_{eff}), and the proton energy difference between the geometric peak and the reaction threshold ($E_p - E_T$). The results are presented as a family of curves in Figure 1.

If one assumes that the cross section is given by:

$$(15) \quad \sigma = \text{const} \left(\frac{E - E_T}{E^5} \right)^{1/2}$$

Or, equally well, if one introduces the slowly varying constant $1/E^{5/2}$ under the integral sign of equations (10) and (11), then integration of these equations gives results that can be shown to be identical to the expressions given by Snowden and Whitehead² for Case I; they have made no mention of Case II. Proceeding as above, the derivative in the region of the peak leads to:

$$\frac{1}{2} = \frac{1}{2} \left(\frac{1}{2} + \frac{1}{2} \right) = 1 \quad (22)$$

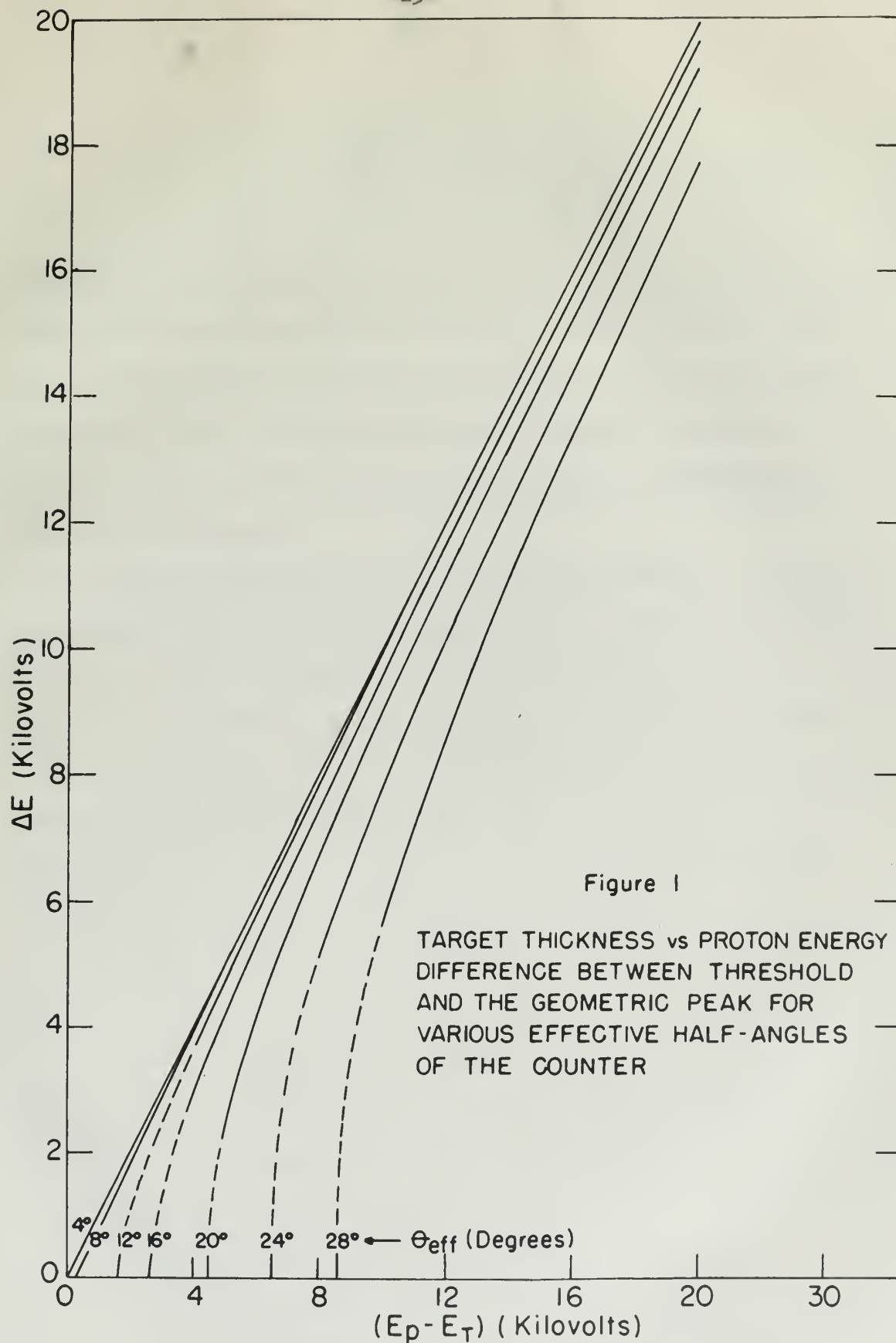
$$\frac{1}{2} \left[\frac{1}{2} \left(\frac{1}{2} + \frac{1}{2} \right) + \frac{1}{2} \left(\frac{1}{2} + \frac{1}{2} \right) \right] = 1 \quad (23)$$

$$\frac{1}{2} \left[\frac{1}{2} \left(\frac{1}{2} + \frac{1}{2} \right) + \frac{1}{2} \left(\frac{1}{2} + \frac{1}{2} \right) \right] = 1 \quad (24)$$

The correlation function $\langle \psi(t) \psi(0) \rangle$ is calculated by using the results in Table I for various values of the parameter β . The results are shown in Figure 1. The correlation function $\langle \psi(t) \psi(0) \rangle$ is calculated by using the results in Table I for various values of the parameter β . The results are shown in Figure 1. The correlation function $\langle \psi(t) \psi(0) \rangle$ is calculated by using the results in Table I for various values of the parameter β . The results are shown in Figure 1.

$$\frac{1}{2} \left(\frac{1}{2} + \frac{1}{2} \right) = 1 \quad (25)$$

The correlation function $\langle \psi(t) \psi(0) \rangle$ is calculated by using the results in Table I for various values of the parameter β . The results are shown in Figure 1. The correlation function $\langle \psi(t) \psi(0) \rangle$ is calculated by using the results in Table I for various values of the parameter β . The results are shown in Figure 1. The correlation function $\langle \psi(t) \psi(0) \rangle$ is calculated by using the results in Table I for various values of the parameter β . The results are shown in Figure 1.



$$(16) \quad \Delta E \approx \frac{E_p - E_T - K}{1 - 5K/E_p} \approx E_p - E_T - K$$

in close agreement with equation (14). This is not surprising, since there is but little variation in the factor $(1/E^{5/2})$ over the relatively small range of energy being considered. Since these results add nothing new to the results previously obtained, the rather lengthy manipulations required for confirmation of the statements just made are omitted.

Equation (14) reduces to the result given by Hanson, Taschek, and Williams¹ when θ is small, namely:

$$(17) \quad \Delta E \approx E_p - E_T.$$

VII. PROTON ENERGY RESOLUTION

The result arrived at in equation (14) is based upon the assumption of an incident monergic proton beam with no proton straggling within the target. The effects will now be considered of an initial energy spread and straggling within the target.

The Rockefeller generator has an effective energy spread of about 0.075 percent with the entrance and exit slits set at 1.0 mm width⁸. Several microamperes of beam current are available with this energy definition. Better energy resolution may be obtained at the expense of beam current by using a narrower slit width.

In order to calculate the straggling it is necessary to know the stopping power (energy loss per unit weight per unit area). Bethe's^{9,10} treatment of energy loss, based upon the Born approximation, after correction for K shell binding, leads to the following equation in the nonrelativistic case:

$$(18) \quad -\frac{dE}{dX} = \frac{4\pi e^4 z^2 N}{mv^2} \left[Z \ln \left(\frac{2mv^2}{I} \right) - C_K \right]$$

where

- ze = charge of the incident particle
- v = velocity of the incident particle
- Z = the nuclear charge of the material
- m = electronic mass
- I = average excitation potential of the atom
- N = number of atoms per cm³ of the material
- C_K = correction term to account for binding in K shell.

This equation as it stands gives the energy loss per unit path length. This equation is used to obtain the stopping power of lithium relative to beryllium for which the absolute value of stopping power is well known¹⁰. This immediately gives:

$$(19) \quad \frac{-\frac{dE}{d(\rho X)}_{Li}}{-\frac{dE}{d(\rho X)}_{Be}} = \frac{W_o \left[Z \ln \left(\frac{2mv^2}{I} \right) - C_k \right]}{W \left[Z_o \ln \left(\frac{2mv^2}{I_o} \right) - C_{k_o} \right]} = 1.09$$

where ρ = density, W = atomic weight, and the subscript "o" denotes the standard which in this case is beryllium. The calculation follows:

$$\text{Relative stopping power} = \frac{B/W}{B_o/W_o}$$

where B and B_o are the quantities within the brackets of numerator and denominator, respectively.

$$2mv^2 = \left(\frac{hm}{M} \right) \left(\frac{Mv^2}{2} \right) = \frac{E_p}{459}$$

where M and E_p are the mass and energy of the proton, respectively.

$$\text{Taking } E_p = 1900 \text{ kev} = 1.9 \times 10^6 \text{ ev,}$$

$$\ln \left(\frac{E_p}{459} \right) = \ln 4139 = 8.324$$

This equation is of course the same as we will
write down. This equation is used to obtain the
of the equation to obtain the value of
the equation is of course the same as we will

$$\frac{\left[\frac{1}{2} \left(\frac{1}{2} \right) \right]}{\left[\frac{1}{2} \left(\frac{1}{2} \right) \right]} = \frac{\frac{1}{2} \left(\frac{1}{2} \right)}{\frac{1}{2} \left(\frac{1}{2} \right)} \quad (11)$$

where $\frac{1}{2}$ is the value of the equation and the
the equation is of course the same as we will

$$\frac{1}{2}$$

where $\frac{1}{2}$ is the value of the equation and the

$$\frac{1}{2}$$

$$\frac{1}{2} = \frac{1}{2} \left(\frac{1}{2} \right)$$

where $\frac{1}{2}$ is the value of the equation and the

$$\frac{1}{2} = \frac{1}{2} \left(\frac{1}{2} \right)$$

$$\frac{1}{2} = \frac{1}{2} \left(\frac{1}{2} \right)$$

$$\ell_n I = \ell_n 34 = 3.526$$

$$\ell_n I_0 = \ell_n 60.4 = 4.101$$

The above I values are from Table 4, reference (9).

$$C_k \simeq C_{k_0} = 0.405 \quad (\text{Table II-1, reference (10)}).$$

Therefore,

$$\frac{B}{B_0} = \frac{14.394 - 0.405}{16.892 - 0.405} = 0.8485.$$

$$\text{Rel. Stop. Pwr (Li to Be)} = \frac{W_0}{W} (0.8485) = \frac{9.015}{7.018} (0.8485) = 1.09$$

Using the value 144 for the absolute stopping power of beryllium for 1900-kev protons (Table III-7, reference (10)), one obtains for lithium:

$$\text{Stopping Power (Li)} = 144 \times 1.09 = 157 \frac{\text{kev cm}^2}{\text{mg}}$$

An initially homogeneous beam of protons, after passing through a target of thickness t will have an energy distribution with a standard deviation Ω given by¹¹,

[illegible]

$$m_1 + m_2 = 2m$$

• (1987) *Journal of the American Academy of Child and Adolescent Psychiatry*, 26: 101-107.

$$\nabla f = (f_x, f_y) = \left(\frac{\partial f}{\partial x}, \frac{\partial f}{\partial y} \right) = (2x - 2, 2y - 2) = (0, 0) \Rightarrow x = 1, y = 1 \Rightarrow (1, 1)$$

1. The first step is to identify the problem or question that needs to be answered. This involves understanding the context and the specific information required.

$$(20) \quad \Omega^2 = \frac{4\pi e^4}{M} \left(\frac{Z}{A}\right) t$$

where M and e are the mass and charge of the proton, Z and A are the atomic and mass numbers of the target element, respectively. The thickness t is in weight per unit area.

$$(21) \quad \Omega = \sqrt{\frac{2\pi e^4}{M}} \left(\frac{2Z}{A}\right)^{1/2} t^{1/2} = 8.85 \left(\frac{2Z}{A}\right)^{1/2} t^{1/2}$$

where $\frac{2Z}{A} \approx 1$ for all elements except hydrogen.

$$\frac{2Z}{A} (\text{lithium}) = \left(\frac{6}{7}\right)^{1/2} = 0.93.$$

(22) $\Omega = 8.23 t^{1/2}$ for lithium; where Ω is given in kev, and t is in mg/cm^2 .

Since the stopping power of lithium was calculated to be

$$157 \frac{\text{kev cm}^2}{\text{mg}}$$

we may write:

(23) $\Omega = 0.657 (\Delta E)^{1/2}$ where Ω is in kev and ΔE is the target thickness in kev. From this equation, the following table is computed:

$$f\left(\frac{z}{\lambda}\right) \frac{dz}{\lambda} = \frac{1}{\lambda} \quad (10)$$

Let us take a look at the function $f(z)$ for small z and large z . For small z , we have $f(z) \approx \frac{1}{\lambda}$. For large z , we have $f(z) \approx \frac{1}{\lambda} \ln z$. This shows that the function $f(z)$ is not bounded as $z \rightarrow \infty$.

$$f\left(\frac{z}{\lambda}\right) \frac{dz}{\lambda} = \frac{1}{\lambda} \ln z \quad (11)$$

Let us now consider the case $\lambda = 1$. Then we have

$$f(z) = \frac{1}{z} \ln z$$

$$f(z) = \frac{1}{z} \ln z \quad (12)$$

Let us now

consider the case $\lambda = 1$. Then we have

$$\frac{1}{z} \ln z$$

Let us now

$$f(z) = \frac{1}{z} \ln z \quad (13)$$

Let us now consider the case $\lambda = 1$. Then we have

Let us now

$\Delta E(\text{kev})$	(kev)	$2 \Gamma_s(\text{kev})$
20	2.94	6.94
15	2.54	5.98
10	2.08	4.90
5	1.47	3.46
4	1.31	3.09
3	1.14	2.69
2	0.93	2.19
1	0.66	1.55
0.5	0.46	1.08

Assuming a normal distribution, the half-width at half maximum (Γ_s) is given by:

$$\Gamma_s = 1.178 \Omega = 0.774 (\Delta E)^{1/2}.$$

The value of $2 \Gamma_s$ is given in the above table for ready comparison with the proton energy spread of the beam, which is about 1.4 kev, for an 0.075 percent energy definition.

It is now desired to determine the minimum value of target thickness for which equation (14) may be expected to be valid when threshold is to be determined by extrapolating the linear portion of the yield curve to the axis. It is unlikely that a precise theoretical treatment can be given. However, an approximate value for this

λ	λ	λ
0.1	0.1	0.1
0.2	0.2	0.2
0.3	0.3	0.3
0.4	0.4	0.4
0.5	0.5	0.5
0.6	0.6	0.6
0.7	0.7	0.7
0.8	0.8	0.8
0.9	0.9	0.9
1.0	1.0	1.0

... ..

... ..

$$f(x) = 1.27x - 0.07x^2$$

The value of $f(x)$ is given in the table for each

... ..

... ..

It is now desired to determine the function $f(x)$ at each

... ..

... ..

... ..

... ..

minimum thickness may be obtained by qualitative arguments based upon some rather crude assumptions, in the following manner.

The geometric peak is treated as a resonance peak with full width at half maximum of the order of $1.4 (E_p - E_T)$. It is shown (Section 3D of reference (9)) that for a resolution equal to or less than the width of half maximum of the resonance peak, the main effect is to depress the peak without changing the slope of the linear portion of the curve. Applying this condition to the geometric peak for a resolution of 2Γ , it follows that for

$$\Gamma < 0.7 \Delta E < 0.7(E_p - E_T)$$

extrapolation to the axis of the linear portion of the rise curve should still give a good value of the reaction threshold. Although the peak has been depressed, there will be no appreciable shift in peak position, inasmuch as the geometric peak is only slightly asymmetrical. Thus, the value of $(E_p - E_T)$ obtained by extrapolation is essentially the same value as would have been obtained with no resolution, and equation (14) will be valid.

The resolution (2Γ) used in the foregoing discussion is the resultant of energy spread in the beam and straggling in the target and will be of the order of the larger of these two resolutions, considered separately. A slightly better value is obtained if it is assumed that these two resolutions add as Gaussians:

$$\Gamma^2 = \Gamma_s^2 + \Gamma_1^2$$

where Γ_1 is the half-width at half maximum of the energy distribution in the beam. Actually, the shape of the energy distribution in the beam is largely dependent upon the exit slit width of the magnetic analyzer (private communication with W. M. Preston), departing from an approximate Gaussian as the slit width is decreased.

Applying the foregoing results to the specific case of a 2-kev target thickness and a 1-mm slit width gives:

$$2\Gamma = [(2.19)^2 + (1.4)^2]^{1/2} = 2.6 \text{ kev.}$$

Since $\Gamma = 1.3$ kev, the condition for validity of equation (14)

$$\Gamma < 0.7 \Delta E \quad \text{becomes}$$

$$\Gamma < 1.4 \text{ kev,}$$

and this inequality holds for the conditions stated.

The conclusion to be drawn from the foregoing is that equation (14) will be valid for target thicknesses of about 2 kev minimum, when the threshold is determined by extrapolation and slit widths of 1 mm are used on the Rockefeller generator.

For $\Gamma > 0.7 (E_p - E_T)$, extrapolation to the axis gives an apparent threshold energy E_T' which is less than E_T since the slope of the curve is decreased. Assuming that the peak position is not

shifted because of resolution, equation (14) becomes:

$$(25) \quad \Delta E = E_p - E_T - K = E_p - E_T' - K - \delta E_T$$

where δE_T is the difference between the true and apparent threshold. This could be determined experimentally for various values of resolution and target thickness. It is apparent, however, that equation (14) may still be used with reasonable results if the position of E_T is accurately known. An accurate method for determining the absolute value of E_T is to measure the yield over the "rise" portion of the geometric peak of a target which is several times thicker than the proton energy resolution of the beam ($\Delta E \sim 20$ kev), using an effective half-angle of the counter, such that $E_0 - E_T \sim 4$ kev. Equation (13a) then applies over the lower portion of the curve where the shape is not affected by the relatively small resolution.

$$N_c \propto (E_0 - E_T)^{3/2}$$

A plot of $N_c^{2/3}$ should thus be linear and its extrapolation to the axis should give an accurate value of E_T . The extreme lower portion of the yield curve must of course be neglected as it has been distorted by the incident proton energy spread.

VIII. THE CALIBRATED LONG COUNTER

The use of a calibrated long counter for determining the thickness of lithium targets is mentioned by Hanson, Taschek, and Williams¹. Aging of the target caused by oxidation, contamination, and the like causes the geometric peak to shift toward higher proton energies, since the total number of atoms has increased. However, the yield at proton energies well above threshold is essentially the same for either the fresh or the aged target, since the number of lithium atoms has not changed while the geometric effects tend to disappear with increasing proton energy. This is attributed to the fact that at proton energies greater than E_L , the neutrons are emitted more nearly isotropically in the laboratory, and the distribution of neutron energies is more nearly uniform over the face of the counter. The change in the shape of the yield curve as a target ages is clearly shown in Figure 17 of reference (1).

It is important to note that target thickness as obtained by a calibrated counter may be used for determining the number of target atoms for either a fresh or aged target. However, the target thickness for purposes of determining the neutron resolution (arising from this target thickness) can be obtained with a calibrated counter only for a fresh target. Conversely, the "rise" method gives target thickness for purposes of determining the neutron resolution (arising from target thickness) for both fresh or aged targets; whereas it leads

to a determination of the number of target (lithium) atoms only for fresh targets. Hence, the necessity of using fresh targets is apparent when one desires to calibrate a counter in terms of counting rate per unit target thickness, if thickness is determined by the rise method for the purpose of calibration.

A measurement of the thickness of a fresh target by the "rise" method followed by a measurement of the yield at a proton energy above 1930 kev in a region where the cross section is nearly constant serves to calibrate the counter in terms of counting rate per unit target thickness. One may select a region of nearly constant cross section either above or below the 2.24-Mev resonance. The region above the peak should give better results as the geometric effect is less pronounced than in the region below the peak.

A calculation will be made to determine the linearity of neutron yield with respect to target thickness for various counter positions for an incident proton energy (E_0) of 1960 kev. This particular value is selected not only because the cross section will be nearly constant for all possible E values within targets of thickness 0 to 30 kev, but also because equation (8f) will apply throughout since $E > E_L$ for all possible E values within the target.

$$(8f) \quad N_0 = Z \int_{E_0 - \Delta E}^{E_0} G_3 \sigma \, dE \dots \dots \dots E > E_L$$

and since σ is nearly constant:

$$(26) \quad N_C = Z \sigma \int_{E_0 - \Delta E}^{E_0} G_3 dE.$$

As the proton energy increases, G_3 approaches a limit which is constant for a given half-angle of the counter. Thus, the counting rate (N_C) approaches $(\sigma Z G_3) \Delta E = \text{const } \Delta E$.

If, however, we evaluate N_C at $E_0 = 1960$ kev,

$$(27) \quad N_C = \frac{\sigma Z}{2} \int_{E_0 - \Delta E}^{E_0} \left[1 - \cos \theta \left\{ 1 - \frac{m_1 m_3}{m_2 m_4} \sin^2 \theta \left(\frac{E}{E - E_T} \right) \right\}^{1/2} \right. \\ \left. + \sin^2 \theta \left(\frac{m_1 m_3}{m_2 m_4} \right)^{1/2} \left(\frac{E}{E - E_T} \right)^{1/2} \right] dE$$

Another form of the expression for G_3 is used here (equation 36c of Appendix A):

$$\frac{m_1 m_3}{m_2 m_4} \sim 0.02 \quad (\sin \theta)_{\max}^2 \sim 0.25 \quad \frac{E}{E - E_T} \sim 25$$

Therefore:

and after it is well known that the following identity holds:

$$\int_{-\infty}^{\infty} \frac{f(x)}{x^2} dx = \int_{-\infty}^{\infty} \frac{f(x)}{x^2} dx \quad (20)$$

is the Fourier transform of the function $f(x)$ and the function $f(x)$ is given by the formula:

$$f(x) = \int_{-\infty}^{\infty} \frac{f(x)}{x^2} dx \quad (21)$$

where $f(x)$ is the function $f(x)$ and the function $f(x)$ is given by the formula:

$$f(x) = \int_{-\infty}^{\infty} \frac{f(x)}{x^2} dx \quad (22)$$

where $f(x)$ is the function $f(x)$ and the function $f(x)$ is given by the formula:

$$f(x) = \int_{-\infty}^{\infty} \frac{f(x)}{x^2} dx \quad (23)$$

where $f(x)$ is the function $f(x)$ and the function $f(x)$ is given by the formula:

$$f(x) = \int_{-\infty}^{\infty} \frac{f(x)}{x^2} dx \quad (24)$$

where $f(x)$ is the function $f(x)$ and the function $f(x)$ is given by the formula:

$$f(x) = \int_{-\infty}^{\infty} \frac{f(x)}{x^2} dx \quad (25)$$

where $f(x)$ is the function $f(x)$ and the function $f(x)$ is given by the formula:

$$\left[\frac{m_1 m_3}{m_2 m_4} \sin^2 \theta \left(\frac{E}{E - E_T} \right) \right]_{\max} \sim 0.125; \text{ hence, only two terms are}$$

needed in the series expansion of the brackets containing this factor:

$$(28) \quad N_c = \frac{\sigma Z}{2} \left[(1 - \cos \theta) \int_{E_0 - \Delta E}^{E_0} dE + \frac{\cos \theta \sin^2 \theta}{2} \left(\frac{m_1 m_3}{m_2 m_4} \right) \int_{E_0 - \Delta E}^{E_0} \frac{E}{E - E_T} dE \right. \\ \left. + \sin^2 \theta \left(\frac{m_1 m_3}{m_2 m_4} \right)^{1/2} \int_{E_0 - \Delta E}^{E_0} \left(\frac{E}{E - E_T} \right)^{1/2} dE \right]$$

First integral:

$$\int_{E_0 - \Delta E}^{E_0} dE = \Delta E$$

Second integral:

$$\int_{E_0 - \Delta E}^{E_0} \frac{E}{E - E_T} dE = \left[E + E_T \ln(E - E_T) \right]_{E_0 - \Delta E}^{E_0} = \Delta E + E_T \ln \left[\frac{E_0 - E_T}{E_0 - E_T - \Delta E} \right]$$

Third integral:

$$\int_{E_0 - \Delta E}^{E_0} \left(\frac{E}{E - E_T} \right)^{1/2} dE = E_0^{1/2} \int \frac{dE}{(E - E_T)^{1/2}} \quad \text{since } E^{1/2} \text{ is}$$

nearly constant over the range of integration. This is readily integrated:

$$E_0^{1/2} \int_{E_0 - \Delta E}^{E_0} \frac{dE}{(E - E_T)^{1/2}} = 2E_0^{1/2} (E - E_T)^{1/2} \Big|_{E_0 - \Delta E}^{E_0}$$

$$= 2E_0^{1/2} \left[(E_0 - E_T)^{1/2} - (E_0 - E_T - \Delta E)^{1/2} \right]$$

Neglecting all terms except the first two in the expansion of

$\left[(E_0 - E_T) - \Delta E \right]^{1/2}$, one obtains:

$$\int_{E_0 - \Delta E}^{E_0} \frac{E^{1/2}}{(E - E_T)^{1/2}} dE \approx \frac{\Delta E}{(1 - E_T/E_0)^{1/2}}$$

First integral

$$\left. \frac{\partial}{\partial t} \left(\frac{1}{\sqrt{1-v^2/c^2}} \right) \right|_{t=0} = \frac{\partial}{\partial t} \left(\frac{1}{\sqrt{1-v^2/c^2}} \right) \Big|_{t=0} = \frac{\partial}{\partial t} \left(\frac{1}{\sqrt{1-v^2/c^2}} \right) \Big|_{t=0}$$

Second integral

$$\left. \frac{\partial}{\partial t} \left(\frac{1}{\sqrt{1-v^2/c^2}} \right) \right|_{t=0} = \frac{\partial}{\partial t} \left(\frac{1}{\sqrt{1-v^2/c^2}} \right) \Big|_{t=0} = \frac{\partial}{\partial t} \left(\frac{1}{\sqrt{1-v^2/c^2}} \right) \Big|_{t=0}$$

$$\left[\frac{\partial}{\partial t} \left(\frac{1}{\sqrt{1-v^2/c^2}} \right) \right]_{t=0} = \frac{\partial}{\partial t} \left(\frac{1}{\sqrt{1-v^2/c^2}} \right) \Big|_{t=0}$$

So we have the first two integrals of the equation of

$$\frac{\partial}{\partial t} \left(\frac{1}{\sqrt{1-v^2/c^2}} \right) \Big|_{t=0} = \frac{\partial}{\partial t} \left(\frac{1}{\sqrt{1-v^2/c^2}} \right) \Big|_{t=0}$$

$$\frac{\partial}{\partial t} \left(\frac{1}{\sqrt{1-v^2/c^2}} \right) \Big|_{t=0} = \frac{\partial}{\partial t} \left(\frac{1}{\sqrt{1-v^2/c^2}} \right) \Big|_{t=0}$$

$$\begin{aligned}
 (29) \quad N_c = \frac{\sigma Z}{2} \left\{ \left[1 - \cos \theta + \frac{\cos \theta \sin^2 \theta}{2} \left(\frac{m_1 m_3}{m_2 m_L} \right) \right. \right. \\
 \left. \left. + \left(1 - \frac{E_T}{E_0} \right)^{-1/2} \sin^2 \theta \left(\frac{m_1 m_3}{m_2 m_L} \right)^{1/2} \right] \Delta E \right. \\
 \left. + \frac{\cos \theta \sin^2 \theta}{2} \left(\frac{m_1 m_3}{m_2 m_L} \right) E_T \ln \left[\frac{E_0 - E_T}{E_0 - E_T - \Delta E} \right] \right\} \\
 (30) \quad N_c = \frac{\sigma Z}{2} \left\{ \left[1 - \cos \theta + 0.01032 \cos \theta \sin^2 \theta + 0.71850 \sin^2 \theta \right] \Delta E \right. \\
 \left. + 19.385 \ln \left(\frac{78}{78 - \Delta E} \right) \cos \theta \sin^2 \theta \right\}
 \end{aligned}$$

Equation (30) is evaluated for various θ and various ΔE in Tables VI through VIII, the final results being displayed in Table VIII. From this table, it is seen that the counting rate per unit target thickness is practically constant for any given half-angle of counter. The results expressed in Table VIII are plotted to give the curve of Figure 2. The linearity of counting rate with respect to target thickness for a given half-angle of the counter is displayed in Tables VII (A-H).

$$\left(\frac{\partial \rho}{\partial t} \right)_{\text{eff}} = \frac{\partial^2 \rho}{\partial x^2} + \left[\frac{\partial \rho}{\partial x} + \frac{\partial \rho}{\partial y} \right] \frac{\partial \rho}{\partial x} + \frac{\partial \rho}{\partial y} \frac{\partial \rho}{\partial y} \quad (22)$$

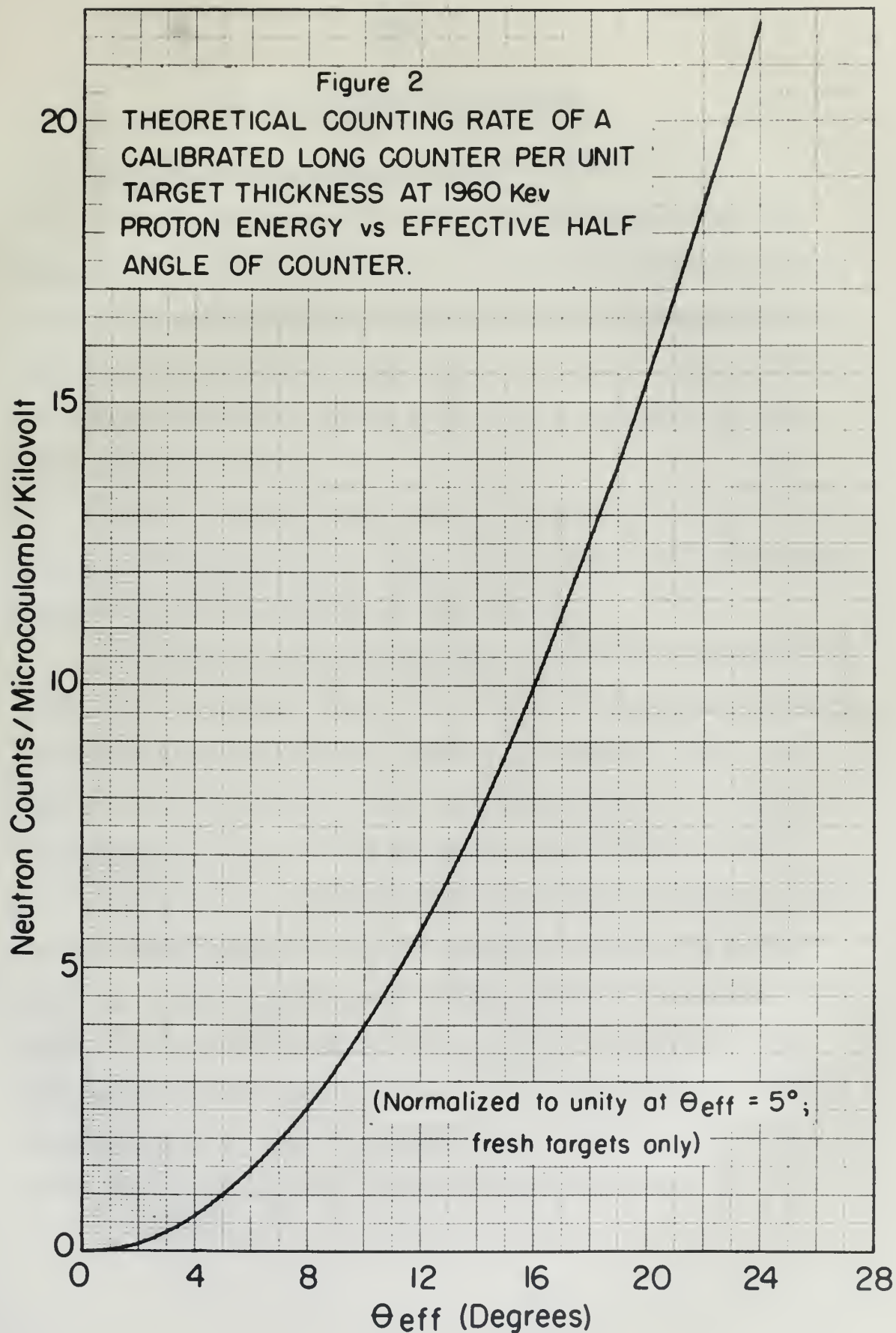
$$E_0 \left[\frac{\partial U(\frac{\partial \pi}{\partial \theta})}{\partial \theta} + E_0 \left(\frac{\partial U}{\partial \theta} \right) \left(\frac{\partial \pi}{\partial \theta} + \pi \right) + \right.$$

$$\left\{ \left[\frac{y_1 - y_2}{x_1 - x_2} \right] = \lim_{x \rightarrow x_0} \frac{y(x) - y(x_0)}{x - x_0} \right.$$

$$\lim_{\lambda \rightarrow 0} \left[\frac{1}{\lambda} \left(\frac{\partial^2 \phi}{\partial x^2} + \frac{\partial^2 \phi}{\partial y^2} \right) + \frac{\partial^2 \phi}{\partial x^2} + \frac{\partial^2 \phi}{\partial y^2} + \frac{\partial^2 \phi}{\partial x^2} + \frac{\partial^2 \phi}{\partial y^2} + \frac{\partial^2 \phi}{\partial x^2} + \frac{\partial^2 \phi}{\partial y^2} \right] = 0 \quad (10)$$

$$\left\{ \begin{array}{l} x^2 + y^2 = r^2 \\ z = h \end{array} \right.$$

1. The Commission has received information from the Government of the United Kingdom that the Government is considering the possibility of introducing legislation to prohibit the export of certain types of goods to the Republic of Ireland.



IX. THE EXPERIMENT AND RESULTS

The purpose of the experiment was:

1. To determine the effective half-angle of the long counter used in this laboratory (7.5-inch paraffin diameter completely shielded with cadmium to reduce background of thermal neutrons) as a function of the distance from the target. With this counter there may be a slight dependence on target thickness; it was desired to check this point.

2. To apply equation (14) to experimental yield curves of targets of several known thicknesses for various counter positions in order to check the validity of this equation.

A convenient method of determining the effective half-angle of the counter for various positions is as follows: Adjust the values of target thickness and counter half-angle to obtain a best fit between the theoretical yield curve³ (equations 12 and 13 apply) and the experimental curve for one relatively large half-angle of the counter. A calibrated counter placed successively at various distances from the target will give a set of relative counting rates per unit target thickness. These relative counting rates, in conjunction with Figure 2, determine a family of possible curves of effective half-angle versus distance from the target. The correct curve is selected from this family by using the value of θ_{eff} found in fitting the theoretical and experimental curves, as mentioned above.

THE HISTORY OF THE UNITED STATES

THE HISTORY OF THE UNITED STATES

I. The history of the United States

CHAPTER I. THE DISCOVERY OF AMERICA
The discovery of America by Christopher Columbus in 1492 is one of the most important events in the history of the world. It opened up a new world of discovery and exploration, and led to the development of the Americas as a major part of the world's population.

II. The early years of the United States

CHAPTER II. THE EARLY YEARS OF THE UNITED STATES
The early years of the United States were marked by a period of rapid growth and expansion. The country was founded on the principles of liberty and democracy, and these principles guided the nation through its early years.

CHAPTER III. THE REVOLUTIONARY WAR

CHAPTER III. THE REVOLUTIONARY WAR
The Revolutionary War was a pivotal moment in the history of the United States. It was a struggle for independence from British rule, and it resulted in the birth of a new nation. The war was fought between the American colonies and the British Empire, and it ended in 1783 with the signing of the Treaty of Paris.

CHAPTER IV. THE CONSTITUTION

CHAPTER IV. THE CONSTITUTION
The Constitution is the foundation of the United States government. It is a document that outlines the structure and powers of the federal government, and it is the basis for all laws and regulations in the country.

CHAPTER V. THE CIVIL WAR

CHAPTER V. THE CIVIL WAR
The Civil War was a period of intense conflict in the United States. It was a struggle between the Northern states and the Southern states, and it resulted in the preservation of the Union. The war was fought from 1861 to 1865, and it ended with the victory of the Union.

CHAPTER VI. THE RECONSTRUCTION

Three lithium targets of various thicknesses were prepared by evaporating the metal in vacuum onto a tantalum backing rotating eccentrically with the beam axis. This apparatus is mounted on the beam exit tube of the Rockefeller generator, making it unnecessary to expose the target to the atmosphere at any time. The need for fresh targets in correlating target thickness by the "rise" method and by calibrated counter is discussed in Section VIII.

An experimental yield curve was determined for each target and for each of the following distances from counter to the target: 39.4, 18, 11, and 7.5 inches. (The 11- and 18-inch yield curves were omitted on the third target because of lack of time.)

The frequency meter normally used for selecting the desired proton energy was inoperative on the day allotted to this experiment. The standby frequency meter, which was used, had an indeterminable frequency drift that caused the proton energy to be in error by a varying amount up to 3 kev maximum. Because of this, the yield curves from two of the three targets were completely unreliable from the viewpoint of this experiment. The remaining target gave reasonably smooth curves, but they are not considered to be accurate enough for determining the effective half-angle by fitting a theoretical curve. The yields obtained are tabulated in Tables I (A-D) and the experimental curves are presented as Figures 3, 4, 5, and 6. In the regions of interest, enough counts were taken so that the standard deviation could be neglected.

A regulated high-voltage supply was the source of the 2250 volts applied to the BF_3 detector. (This voltage corresponds to the center of the plateau for that particular counter.) The counting rate with a Ra-Be standard source on top of the counter was determined at intervals over a period of three days and never varied more than 2.6 percent.

The BF_3 detector was a Model 3 hOE Mark 2, manufactured by Radiation Counter Laboratories. The output pulses were fed through a preamplifier to a Model 100 amplifier, thence to a Model 1060 multiscaler manufactured by the Atomic Instrument Company. The discriminator is an integral part of the complete multiscaler unit.

Counts were taken for an integral number of microcoulombs of charge on the target. If the beam current changed appreciably during a run, the count was repeated.

Background was small enough to be neglected throughout this experiment.

In an attempt to derive from this experiment some information that would be of immediate use to this laboratory, it was decided to proceed with the assumption that equation (14) is valid and to select that particular curve from the family of possible curves of effective half-angle versus distance from the target which would produce the observed shift in peak position at the various counter positions.

Since the yield is slow varying in the vicinity of 1960-kev proton energy, the counting rates are hardly affected by the frequency drift experienced and may be used for all three targets. In Table VIII, it is shown that the counting rate per unit target thickness is independent of target thickness for the counter half-angles used. An average value of counting rate per unit target thickness for the three targets is calculated, and the relative counting rate determined.

There is a great deal of talk about the value of money, but it is not always clear what is meant. Money is a means to an end, and its value is determined by the amount of goods and services it can buy. In this sense, the value of money is relative to the prices of the things it can purchase. If the price of a good falls, the value of money increases, and vice versa. This is why it is important to understand the relationship between money and the things it can buy. Money is not an end in itself, but a means to the end of satisfying our needs and desires. The value of money is therefore determined by the value of the things it can buy. This is the basic principle of the value of money, and it is the foundation of all economic theory.

The value of money is also determined by the amount of money in circulation. If there is too much money, the value of money will fall, and prices will rise. This is called inflation. If there is too little money, the value of money will rise, and prices will fall. This is called deflation. The value of money is therefore determined by the balance between the amount of money in circulation and the amount of goods and services available. This is the basic principle of the value of money, and it is the foundation of all economic theory. The value of money is also determined by the confidence of the public in the money. If the public loses confidence in the money, the value of money will fall, and prices will rise. This is why it is important to maintain the confidence of the public in the money. The value of money is therefore determined by the confidence of the public in the money, and this is the foundation of all economic theory.

TABLE I (A)

Experimental Data
Counter at 00, 39.4 inches from Target

<u>Target</u>	<u>Frequency (Megacycles)</u>	<u>Counts</u>	<u>μCoulombs</u>
No. 2	10.468	48	40
	.470	507	40
	.471	2438	40
	.473	5566	40
	.476	7487	40
	.479	8923	40
	.482	10004	40
	.485	10967	40
	.487	22508	80
	.489	22428	80
	.491	21181	80
	.495	19523	80
	.500	8349	40
	.680	9382	160
No. 1	10.680	6431	80
No. 3	10.680	24297	80

TABLE I

Summary of the results of the tests of the various types of concrete beams under load.

Beam No.	Span, ft.	Load, lb.	Deflection, in.
1	10	10,000	1.0
2	10	20,000	2.0
3	10	30,000	3.0
4	10	40,000	4.0
5	10	50,000	5.0
6	10	60,000	6.0
7	10	70,000	7.0
8	10	80,000	8.0
9	10	90,000	9.0
10	10	100,000	10.0
11	10	110,000	11.0
12	10	120,000	12.0
13	10	130,000	13.0
14	10	140,000	14.0
15	10	150,000	15.0
16	10	160,000	16.0
17	10	170,000	17.0
18	10	180,000	18.0
19	10	190,000	19.0
20	10	200,000	20.0
21	10	210,000	21.0
22	10	220,000	22.0
23	10	230,000	23.0
24	10	240,000	24.0
25	10	250,000	25.0
26	10	260,000	26.0
27	10	270,000	27.0
28	10	280,000	28.0
29	10	290,000	29.0
30	10	300,000	30.0
31	10	310,000	31.0
32	10	320,000	32.0
33	10	330,000	33.0
34	10	340,000	34.0
35	10	350,000	35.0
36	10	360,000	36.0
37	10	370,000	37.0
38	10	380,000	38.0
39	10	390,000	39.0
40	10	400,000	40.0
41	10	410,000	41.0
42	10	420,000	42.0
43	10	430,000	43.0
44	10	440,000	44.0
45	10	450,000	45.0
46	10	460,000	46.0
47	10	470,000	47.0
48	10	480,000	48.0
49	10	490,000	49.0
50	10	500,000	50.0
51	10	510,000	51.0
52	10	520,000	52.0
53	10	530,000	53.0
54	10	540,000	54.0
55	10	550,000	55.0
56	10	560,000	56.0
57	10	570,000	57.0
58	10	580,000	58.0
59	10	590,000	59.0
60	10	600,000	60.0
61	10	610,000	61.0
62	10	620,000	62.0
63	10	630,000	63.0
64	10	640,000	64.0
65	10	650,000	65.0
66	10	660,000	66.0
67	10	670,000	67.0
68	10	680,000	68.0
69	10	690,000	69.0
70	10	700,000	70.0
71	10	710,000	71.0
72	10	720,000	72.0
73	10	730,000	73.0
74	10	740,000	74.0
75	10	750,000	75.0
76	10	760,000	76.0
77	10	770,000	77.0
78	10	780,000	78.0
79	10	790,000	79.0
80	10	800,000	80.0
81	10	810,000	81.0
82	10	820,000	82.0
83	10	830,000	83.0
84	10	840,000	84.0
85	10	850,000	85.0
86	10	860,000	86.0
87	10	870,000	87.0
88	10	880,000	88.0
89	10	890,000	89.0
90	10	900,000	90.0
91	10	910,000	91.0
92	10	920,000	92.0
93	10	930,000	93.0
94	10	940,000	94.0
95	10	950,000	95.0
96	10	960,000	96.0
97	10	970,000	97.0
98	10	980,000	98.0
99	10	990,000	99.0
100	10	1,000,000	100.0

TABLE I(B)

Experimental Data
Counter at 0°, 18 inches from Target

<u>Target</u>	<u>Frequency (Megacycles)</u>	<u>Counts</u>	<u>μCoulombs</u>
No. 2	10.478	206	40
	.481	4017	40
	.482	9937	40
	.484	20669	40
	.486	26345	40
	.488	33213	40
	.490	39450	40
	.492	41834	40
	.494	43471	40
	.496	44300	40
	.498	45990	40
	.500	45287	40
	.502	44162	40
	.510	34790	40
	.680	17534	80
No. 1	10.680	25320	80
No. 3	10.680	-	-

(b)(1) (b)(2) (b)(3)

UNITED STATES DEPARTMENT OF JUSTICE
FEDERAL BUREAU OF INVESTIGATION

DATE	TIME	LOCATION	REMARKS
10/10/70	10:00	NEW YORK	1. 100
10/11/70	10:00	NEW YORK	2. 100
10/12/70	10:00	NEW YORK	3. 100
10/13/70	10:00	NEW YORK	4. 100
10/14/70	10:00	NEW YORK	5. 100
10/15/70	10:00	NEW YORK	6. 100
10/16/70	10:00	NEW YORK	7. 100
10/17/70	10:00	NEW YORK	8. 100
10/18/70	10:00	NEW YORK	9. 100
10/19/70	10:00	NEW YORK	10. 100
10/20/70	10:00	NEW YORK	11. 100
10/21/70	10:00	NEW YORK	12. 100
10/22/70	10:00	NEW YORK	13. 100
10/23/70	10:00	NEW YORK	14. 100
10/24/70	10:00	NEW YORK	15. 100
10/25/70	10:00	NEW YORK	16. 100
10/26/70	10:00	NEW YORK	17. 100
10/27/70	10:00	NEW YORK	18. 100
10/28/70	10:00	NEW YORK	19. 100
10/29/70	10:00	NEW YORK	20. 100
10/30/70	10:00	NEW YORK	21. 100
10/31/70	10:00	NEW YORK	22. 100
11/01/70	10:00	NEW YORK	23. 100
11/02/70	10:00	NEW YORK	24. 100
11/03/70	10:00	NEW YORK	25. 100
11/04/70	10:00	NEW YORK	26. 100
11/05/70	10:00	NEW YORK	27. 100
11/06/70	10:00	NEW YORK	28. 100
11/07/70	10:00	NEW YORK	29. 100
11/08/70	10:00	NEW YORK	30. 100
11/09/70	10:00	NEW YORK	31. 100
11/10/70	10:00	NEW YORK	32. 100
11/11/70	10:00	NEW YORK	33. 100
11/12/70	10:00	NEW YORK	34. 100
11/13/70	10:00	NEW YORK	35. 100
11/14/70	10:00	NEW YORK	36. 100
11/15/70	10:00	NEW YORK	37. 100
11/16/70	10:00	NEW YORK	38. 100
11/17/70	10:00	NEW YORK	39. 100
11/18/70	10:00	NEW YORK	40. 100
11/19/70	10:00	NEW YORK	41. 100
11/20/70	10:00	NEW YORK	42. 100
11/21/70	10:00	NEW YORK	43. 100
11/22/70	10:00	NEW YORK	44. 100
11/23/70	10:00	NEW YORK	45. 100
11/24/70	10:00	NEW YORK	46. 100
11/25/70	10:00	NEW YORK	47. 100
11/26/70	10:00	NEW YORK	48. 100
11/27/70	10:00	NEW YORK	49. 100
11/28/70	10:00	NEW YORK	50. 100
11/29/70	10:00	NEW YORK	51. 100
11/30/70	10:00	NEW YORK	52. 100
12/01/70	10:00	NEW YORK	53. 100
12/02/70	10:00	NEW YORK	54. 100
12/03/70	10:00	NEW YORK	55. 100
12/04/70	10:00	NEW YORK	56. 100
12/05/70	10:00	NEW YORK	57. 100
12/06/70	10:00	NEW YORK	58. 100
12/07/70	10:00	NEW YORK	59. 100
12/08/70	10:00	NEW YORK	60. 100
12/09/70	10:00	NEW YORK	61. 100
12/10/70	10:00	NEW YORK	62. 100
12/11/70	10:00	NEW YORK	63. 100
12/12/70	10:00	NEW YORK	64. 100
12/13/70	10:00	NEW YORK	65. 100
12/14/70	10:00	NEW YORK	66. 100
12/15/70	10:00	NEW YORK	67. 100
12/16/70	10:00	NEW YORK	68. 100
12/17/70	10:00	NEW YORK	69. 100
12/18/70	10:00	NEW YORK	70. 100
12/19/70	10:00	NEW YORK	71. 100
12/20/70	10:00	NEW YORK	72. 100
12/21/70	10:00	NEW YORK	73. 100
12/22/70	10:00	NEW YORK	74. 100
12/23/70	10:00	NEW YORK	75. 100
12/24/70	10:00	NEW YORK	76. 100
12/25/70	10:00	NEW YORK	77. 100
12/26/70	10:00	NEW YORK	78. 100
12/27/70	10:00	NEW YORK	79. 100
12/28/70	10:00	NEW YORK	80. 100
12/29/70	10:00	NEW YORK	81. 100
12/30/70	10:00	NEW YORK	82. 100
12/31/70	10:00	NEW YORK	83. 100
1/01/71	10:00	NEW YORK	84. 100
1/02/71	10:00	NEW YORK	85. 100
1/03/71	10:00	NEW YORK	86. 100
1/04/71	10:00	NEW YORK	87. 100
1/05/71	10:00	NEW YORK	88. 100
1/06/71	10:00	NEW YORK	89. 100
1/07/71	10:00	NEW YORK	90. 100
1/08/71	10:00	NEW YORK	91. 100
1/09/71	10:00	NEW YORK	92. 100
1/10/71	10:00	NEW YORK	93. 100
1/11/71	10:00	NEW YORK	94. 100
1/12/71	10:00	NEW YORK	95. 100
1/13/71	10:00	NEW YORK	96. 100
1/14/71	10:00	NEW YORK	97. 100
1/15/71	10:00	NEW YORK	98. 100
1/16/71	10:00	NEW YORK	99. 100
1/17/71	10:00	NEW YORK	100. 100

TABLE I (G)

Experimental Data
Counter at 0°, 11 inches from Target

<u>Target</u>	<u>Frequency (Megacycles)</u>	<u>Counts</u>	<u>μCoulombs</u>
No. 2	10.478	586	20
	.480	3864	20
	.483	14506	20
	.485	22813	20
	.489	36572	20
	.493	44621	20
	.496	48686	20
	.498	53171	20
	.500	52869	20
	.502	52078	20
	.506	48899	20
	.680	40968	80
No. 1	10.680	64856	80
No. 3	10.680	-	-

(6) T. 2222

Department of
Internal Affairs, T. 2222, as amended

Section	Section	Section (continued)	Section
10	10	10	10
20	20	20	20
30	30	30	30
40	40	40	40
50	50	50	50
60	60	60	60
70	70	70	70
80	80	80	80
90	90	90	90
100	100	100	100
110	110	110	110
120	120	120	120
130	130	130	130
140	140	140	140
150	150	150	150
160	160	160	160
170	170	170	170
180	180	180	180
190	190	190	190
200	200	200	200
210	210	210	210
220	220	220	220
230	230	230	230
240	240	240	240
250	250	250	250
260	260	260	260
270	270	270	270
280	280	280	280
290	290	290	290
300	300	300	300
310	310	310	310
320	320	320	320
330	330	330	330
340	340	340	340
350	350	350	350
360	360	360	360
370	370	370	370
380	380	380	380
390	390	390	390
400	400	400	400
410	410	410	410
420	420	420	420
430	430	430	430
440	440	440	440
450	450	450	450
460	460	460	460
470	470	470	470
480	480	480	480
490	490	490	490
500	500	500	500
510	510	510	510
520	520	520	520
530	530	530	530
540	540	540	540
550	550	550	550
560	560	560	560
570	570	570	570
580	580	580	580
590	590	590	590
600	600	600	600
610	610	610	610
620	620	620	620
630	630	630	630
640	640	640	640
650	650	650	650
660	660	660	660
670	670	670	670
680	680	680	680
690	690	690	690
700	700	700	700
710	710	710	710
720	720	720	720
730	730	730	730
740	740	740	740
750	750	750	750
760	760	760	760
770	770	770	770
780	780	780	780
790	790	790	790
800	800	800	800
810	810	810	810
820	820	820	820
830	830	830	830
840	840	840	840
850	850	850	850
860	860	860	860
870	870	870	870
880	880	880	880
890	890	890	890
900	900	900	900
910	910	910	910
920	920	920	920
930	930	930	930
940	940	940	940
950	950	950	950
960	960	960	960
970	970	970	970
980	980	980	980
990	990	990	990
1000	1000	1000	1000

TABLE I (D)

Experimental Data
Counter at 0°, 7.5 inches from Target

<u>Target</u>	<u>Frequency (Megacycles)</u>	<u>Counts</u>	<u>μCoulombs</u>
No. 2	10.4855	2644	20
	.488	14370	20
	.491	29869	20
	.494	47787	20
	.497	62822	20
	.499	68224	20
	.501	72367	20
	.503	81286	20
	.505	86557	20
	.507	85522	20
	.509	84755	20
	.511	82615	20
	.515	73769	20
	.680	33912	40
No. 1	10.680	49807	40
No. 3	10.680	43949	10

TABLE 1 (C)

Department of
Commerce and Industry, Singapore

Year	Value (in thousands of dollars)	Percentage of total	Year
1950	100.0	100.0	1950
1951	100.0	100.0	1951
1952	100.0	100.0	1952
1953	100.0	100.0	1953
1954	100.0	100.0	1954
1955	100.0	100.0	1955
1956	100.0	100.0	1956
1957	100.0	100.0	1957
1958	100.0	100.0	1958
1959	100.0	100.0	1959
1960	100.0	100.0	1960
1961	100.0	100.0	1961
1962	100.0	100.0	1962
1963	100.0	100.0	1963
1964	100.0	100.0	1964
1965	100.0	100.0	1965
1966	100.0	100.0	1966
1967	100.0	100.0	1967
1968	100.0	100.0	1968
1969	100.0	100.0	1969
1970	100.0	100.0	1970
1971	100.0	100.0	1971
1972	100.0	100.0	1972
1973	100.0	100.0	1973
1974	100.0	100.0	1974
1975	100.0	100.0	1975
1976	100.0	100.0	1976
1977	100.0	100.0	1977
1978	100.0	100.0	1978
1979	100.0	100.0	1979
1980	100.0	100.0	1980
1981	100.0	100.0	1981
1982	100.0	100.0	1982
1983	100.0	100.0	1983
1984	100.0	100.0	1984
1985	100.0	100.0	1985
1986	100.0	100.0	1986
1987	100.0	100.0	1987
1988	100.0	100.0	1988
1989	100.0	100.0	1989
1990	100.0	100.0	1990
1991	100.0	100.0	1991
1992	100.0	100.0	1992
1993	100.0	100.0	1993
1994	100.0	100.0	1994
1995	100.0	100.0	1995
1996	100.0	100.0	1996
1997	100.0	100.0	1997
1998	100.0	100.0	1998
1999	100.0	100.0	1999
2000	100.0	100.0	2000
2001	100.0	100.0	2001
2002	100.0	100.0	2002
2003	100.0	100.0	2003
2004	100.0	100.0	2004
2005	100.0	100.0	2005
2006	100.0	100.0	2006
2007	100.0	100.0	2007
2008	100.0	100.0	2008
2009	100.0	100.0	2009
2010	100.0	100.0	2010
2011	100.0	100.0	2011
2012	100.0	100.0	2012
2013	100.0	100.0	2013
2014	100.0	100.0	2014
2015	100.0	100.0	2015
2016	100.0	100.0	2016
2017	100.0	100.0	2017
2018	100.0	100.0	2018
2019	100.0	100.0	2019
2020	100.0	100.0	2020
2021	100.0	100.0	2021
2022	100.0	100.0	2022
2023	100.0	100.0	2023
2024	100.0	100.0	2024
2025	100.0	100.0	2025
2026	100.0	100.0	2026
2027	100.0	100.0	2027
2028	100.0	100.0	2028
2029	100.0	100.0	2029
2030	100.0	100.0	2030
2031	100.0	100.0	2031
2032	100.0	100.0	2032
2033	100.0	100.0	2033
2034	100.0	100.0	2034
2035	100.0	100.0	2035
2036	100.0	100.0	2036
2037	100.0	100.0	2037
2038	100.0	100.0	2038
2039	100.0	100.0	2039
2040	100.0	100.0	2040
2041	100.0	100.0	2041
2042	100.0	100.0	2042
2043	100.0	100.0	2043
2044	100.0	100.0	2044
2045	100.0	100.0	2045
2046	100.0	100.0	2046
2047	100.0	100.0	2047
2048	100.0	100.0	2048
2049	100.0	100.0	2049
2050	100.0	100.0	2050
2051	100.0	100.0	2051
2052	100.0	100.0	2052
2053	100.0	100.0	2053
2054	100.0	100.0	2054
2055	100.0	100.0	2055
2056	100.0	100.0	2056
2057	100.0	100.0	2057
2058	100.0	100.0	2058
2059	100.0	100.0	2059
2060	100.0	100.0	2060
2061	100.0	100.0	2061
2062	100.0	100.0	2062
2063	100.0	100.0	2063
2064	100.0	100.0	2064
2065	100.0	100.0	2065
2066	100.0	100.0	2066
2067	100.0	100.0	2067
2068	100.0	100.0	2068
2069	100.0	100.0	2069
2070	100.0	100.0	2070
2071	100.0	100.0	2071
2072	100.0	100.0	2072
2073	100.0	100.0	2073
2074	100.0	100.0	2074
2075	100.0	100.0	2075
2076	100.0	100.0	2076
2077	100.0	100.0	2077
2078	100.0	100.0	2078
2079	100.0	100.0	2079
2080	100.0	100.0	2080
2081	100.0	100.0	2081
2082	100.0	100.0	2082
2083	100.0	100.0	2083
2084	100.0	100.0	2084
2085	100.0	100.0	2085
2086	100.0	100.0	2086
2087	100.0	100.0	2087
2088	100.0	100.0	2088
2089	100.0	100.0	2089
2090	100.0	100.0	2090
2091	100.0	100.0	2091
2092	100.0	100.0	2092
2093	100.0	100.0	2093
2094	100.0	100.0	2094
2095	100.0	100.0	2095
2096	100.0	100.0	2096
2097	100.0	100.0	2097
2098	100.0	100.0	2098
2099	100.0	100.0	2099
2100	100.0	100.0	2100

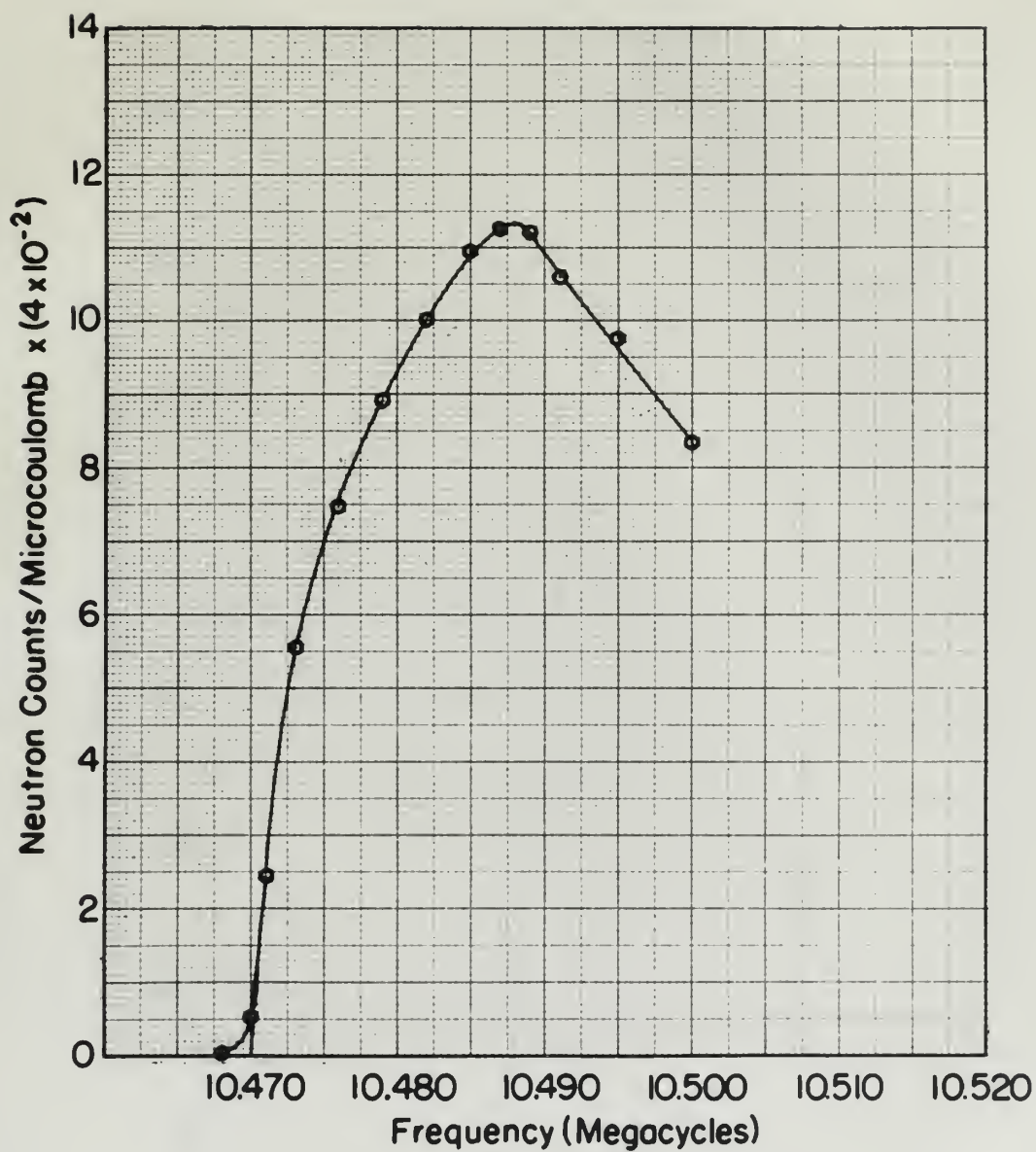


Figure 3

Neutron Yield from $\text{Li}^7 (p,n) \text{Be}^7$

Target Thickness 6.44 Kev

Distance from Target to Counter = 39.4 inches

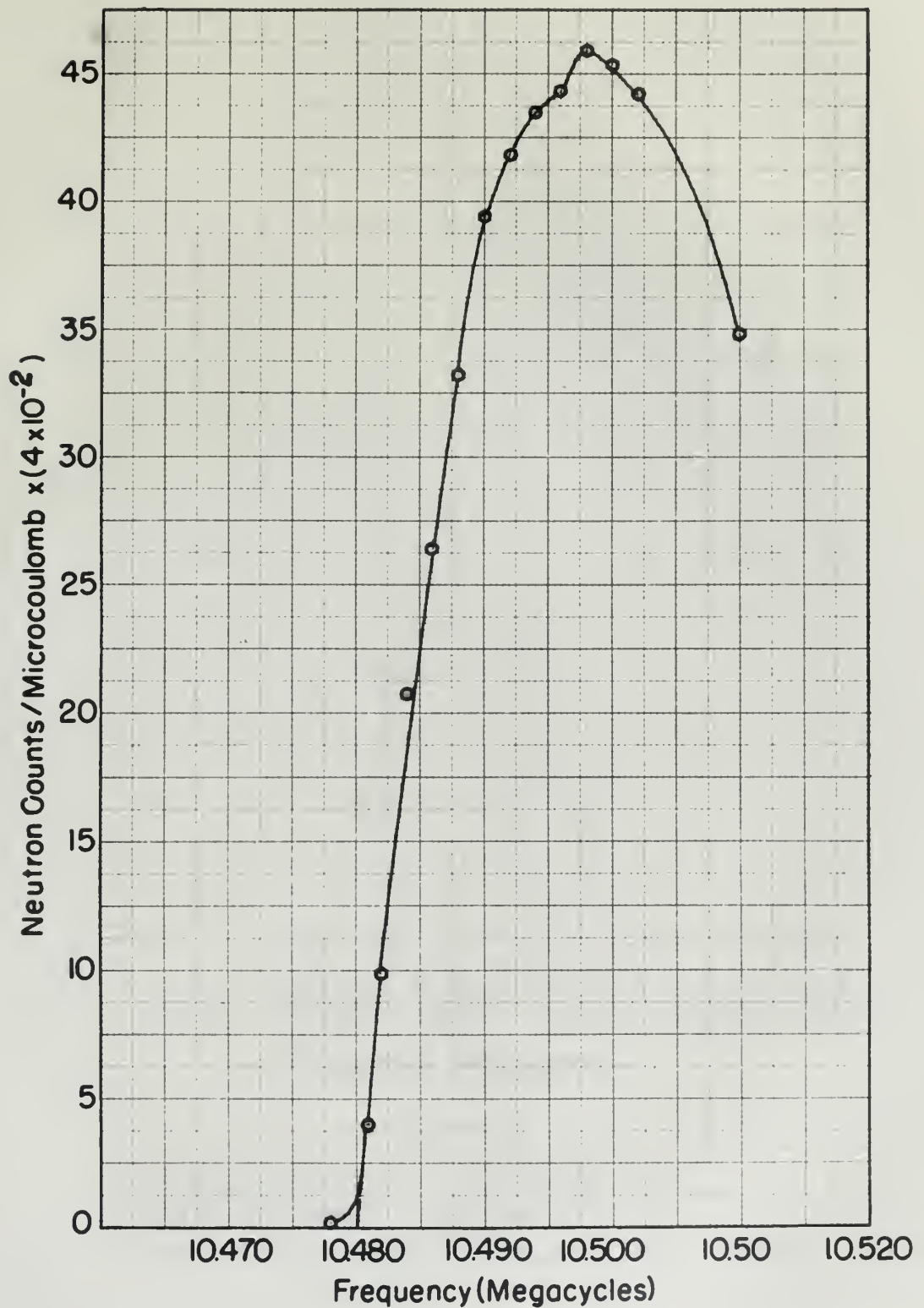


Figure 4

Neutron Yield from $\text{Li}^7(p,n)\text{Be}^7$

Target Thickness 6.44 Kev

Distance from Target to Counter = 18.0 inches

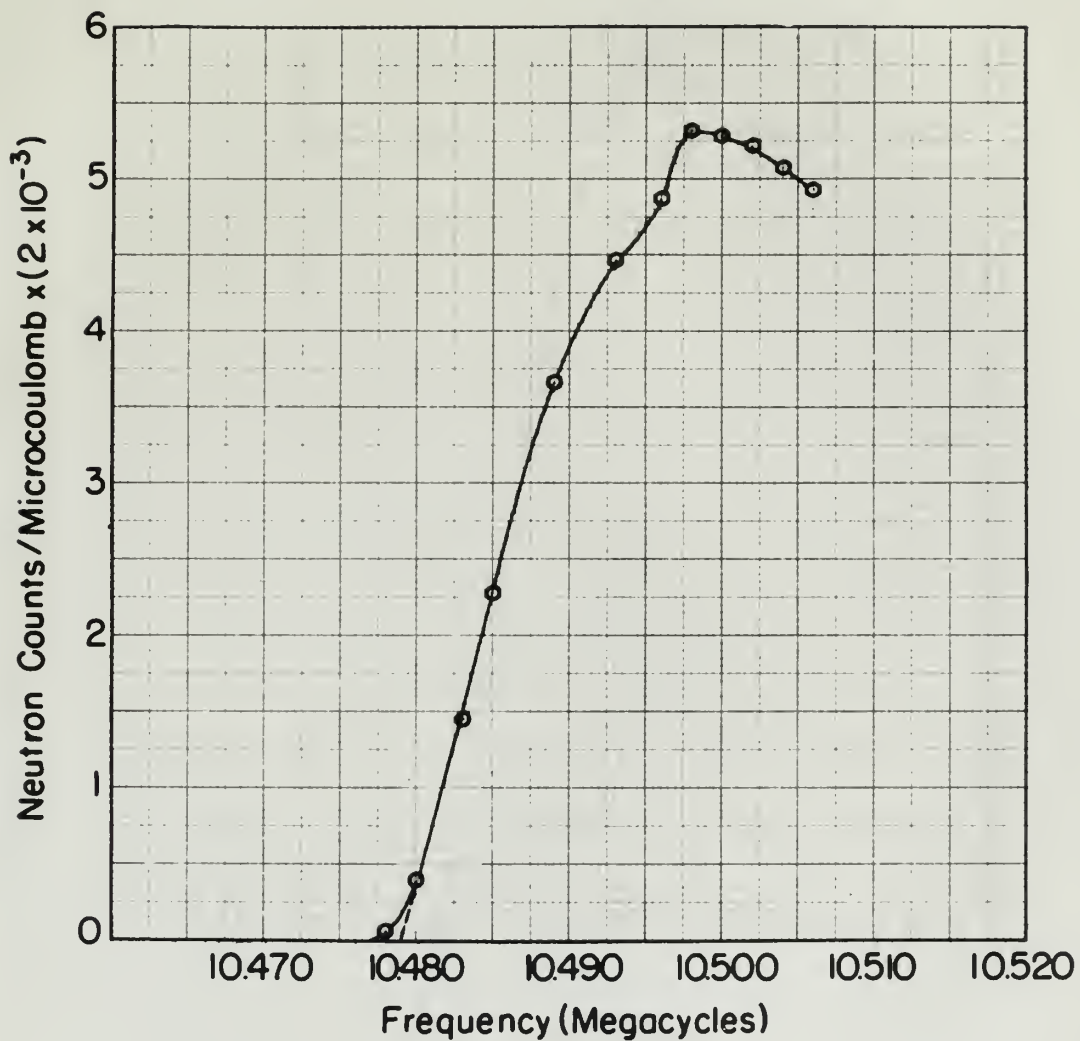


Figure 5

Neutron Yield from $\text{Li}^7 (p,n) \text{Be}^7$

Target Thickness 6.44 Kev

Distance from Target to Counter = 11.0 inches

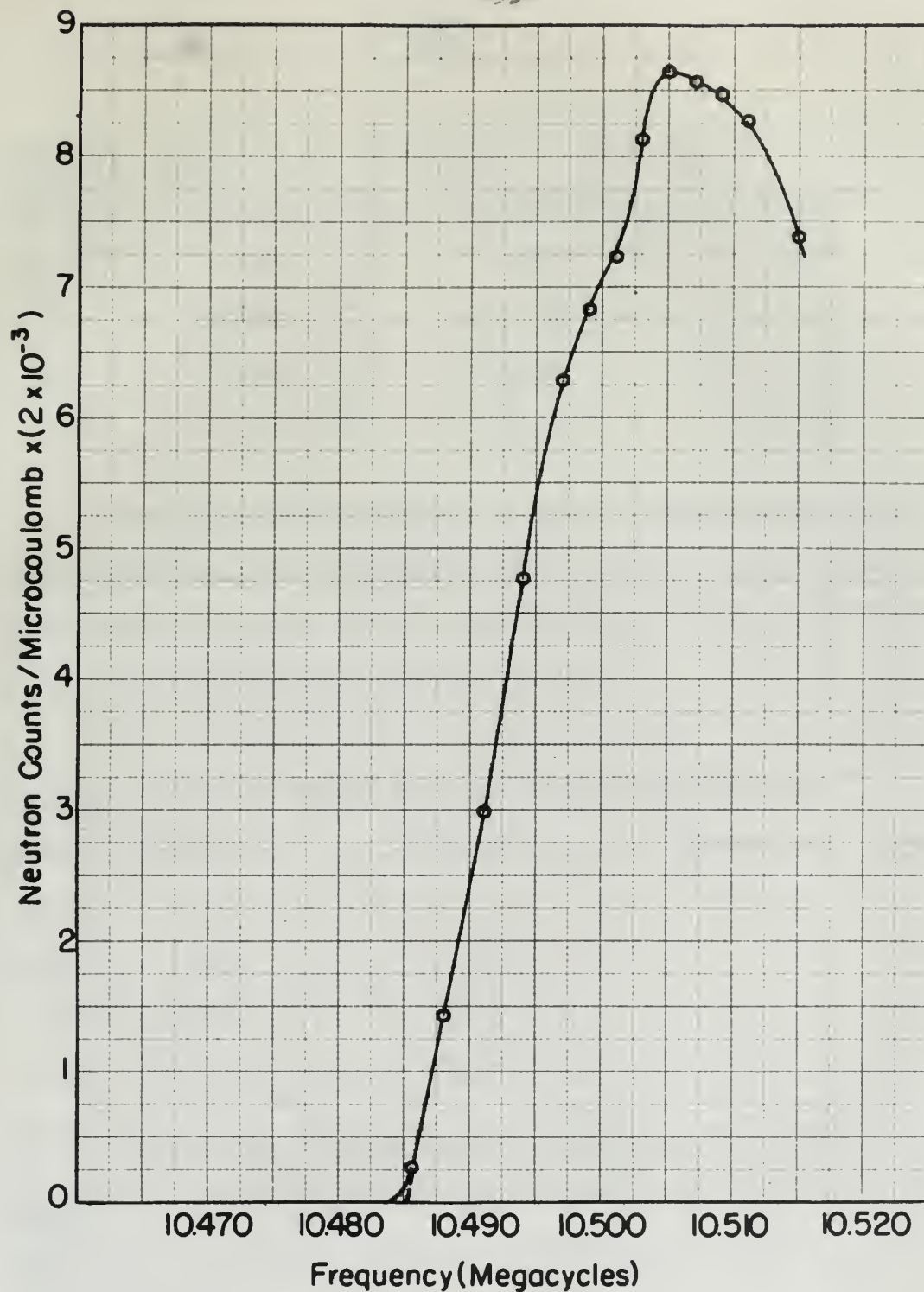


Figure 6

Neutron Yield from $\text{Li}^7(p,n)\text{Be}^7$

Target Thickness 6.44 Kev

Distance from Target to Counter = 7.5 inches

Distance from Target	Counts per 80 μ Coulombs at 1953-keV Proton Energy		
	Target 1	Target 2	Target 3
39.4"	6431	4691	24297
18.0	25320	17534	-
11.0	64856	40968	-
7.5	99614	67824	351592

Since the counting rate per unit target thickness should be constant at any given distance from the target, the number unity is arbitrarily assigned to the values obtaining at 39.4 inches and the ratios calculated with reference to it.

Distance from Target	Relative Counting Rates per Unit Target Thickness			
	Target 1	Target 2	Target 3	Average
39.4"	1	1	1	1
18.0	3.94	3.74	-	3.84
11.0	10.08	8.73	-	9.41
7.5	15.49	14.46	14.47	14.81

These average relative counting rates are maintained but are normalized to fit the curve of Figure 2 so that the effective half-angle has in succession the values 3° , 4° , and 5° at 39.4 inches from the target.

Station from Point 1	Point 1	Point 2	Point 3	Station from Point 3
10.4	6.22	6.97	10.57	
11.0	6.29	7.02	-	
11.5	6.35	7.08	-	
12.0	6.41	7.14	10.63	

From the readings with the level instrument the
 heights of the points from the datum, the mean value
 is calculated and the value obtained is 10.4 inches and
 the value calculated with the level is 11.

Station from Point 1	Point 1	Point 2	Point 3	Station from Point 3
10.4	6.22	6.97	10.57	
11.0	6.29	7.02	-	
11.5	6.35	7.08	-	
12.0	6.41	7.14	10.63	

From the readings with the level instrument the
 heights of the points from the datum, the mean value
 is calculated and the value obtained is 10.4 inches and
 the value calculated with the level is 11.

Counter Distance	Aver. Ratios	Ratio	$\theta^{\circ}_{\text{eff}}$	Ratio	$\theta^{\circ}_{\text{eff}}$	Ratio	$\theta^{\circ}_{\text{eff}}$
39.4"	1	.361	3.0	.63	4.0	1	5
18.0	3.84	1.386	5.8	2.42	7.7	3.84	9.8
11.0	9.41	3.397	9.2	5.93	12.2	9.41	15.5
7.5	14.81	5.346	11.6	9.33	15.4	14.81	19.6

From these values are drawn the three curves of the family of curves of effective half-angle versus distance from the target (Figure 7).

The difference between the peak and threshold positions in kilocycles is taken directly from the yield curves. These frequency differences (ΔF) are converted into proton energy differences by the relation:

$$(31) \quad (E_p - E_T) \text{ kev} = \frac{\delta E}{\delta F} \Delta F$$

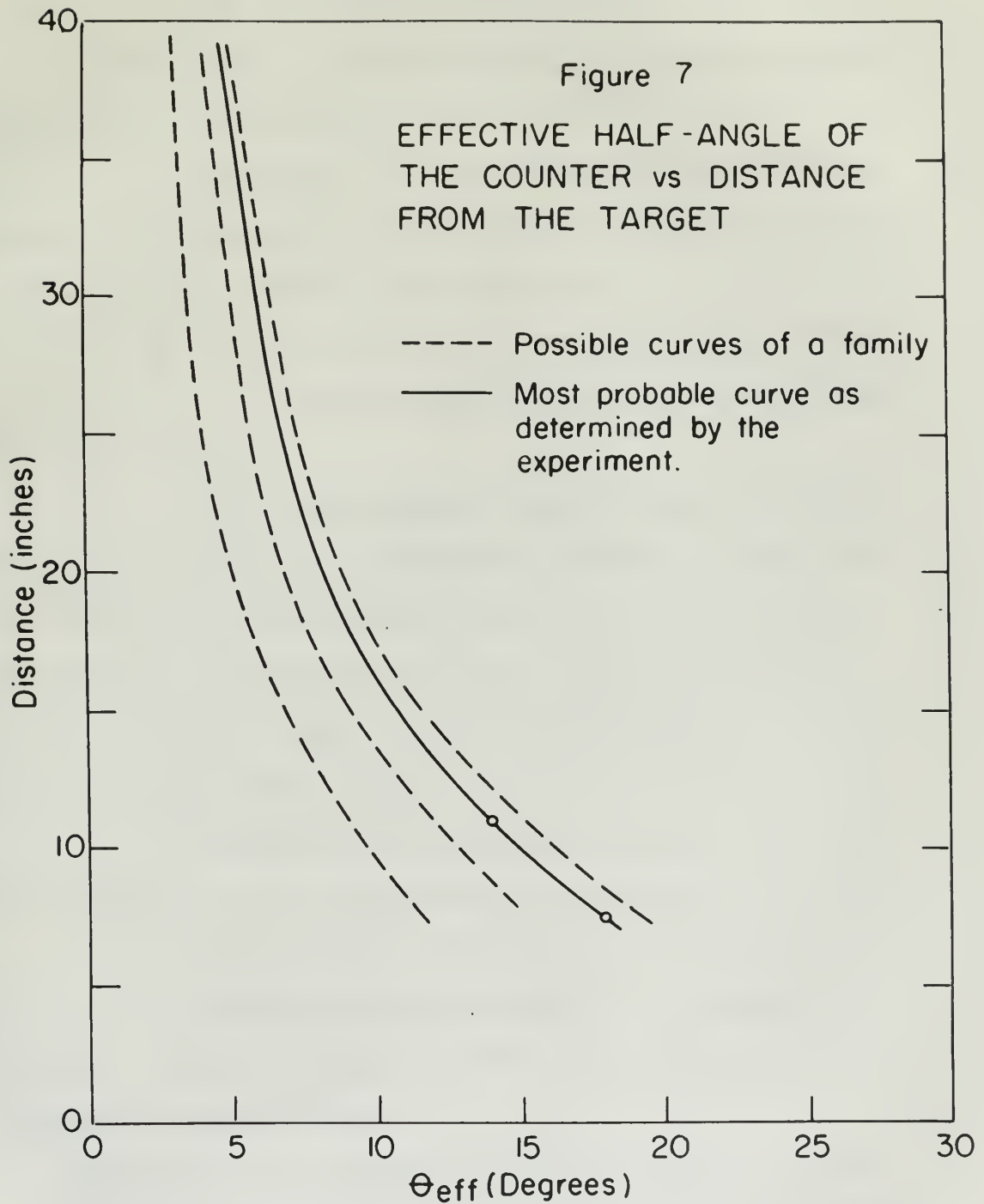
where $\delta E / \delta F = 0.3575 \text{ kev/kc.}$ for ΔF in kilocycles and a proton energy of 1982 kev. Target thickness is taken as the value of the proton energy difference between the peak and threshold ($E_p - E_T$) with the counter at 39.4 inches in accordance with equation (14), since the correction term (K) is negligible in this case. Entering Figure 1 with the value of target thickness ($\Delta E = 6.44 \text{ kev}$), one obtains a value of θ_{eff} for each value of $E_p - E_T$. The results follow:

<u>Distance from Target</u>	<u>$\Delta F(\text{ke})$</u>	<u>$E_p - E_T$</u>	<u>θ_{eff}</u>
39.4"	18	6.44 = ΔE	-
18.0	18	6.44	-
11.0	19	6.80	14°
7.5	20	7.15	18°

The values, $\theta_{\text{eff}} = 14^\circ, 18^\circ$ are plotted on the family of curves in Figure 7. The most probable curve is now drawn through these two points, giving the best value of the effective half-angle of this particular counter for any counter position between 7.5 and 39.4 inches. This curve may be extrapolated to some extent in either direction.

The following table may be of assistance in applying the above results to a long counter with paraffin diameter slightly different from the 7.5-inch diameter used in this laboratory.

<u>Distance (d)</u>	<u>$\tan \theta$ $= 3.75/d$</u>	<u>θ (Actual)</u>	<u>θ_{eff}</u>
39.4"	.09525	5.43°	4.6°
18.0	.20833	11.77°	9.0°
11.0	.34091	18.82°	14.0°
7.5	.50000	26.57°	18.0°



X. APPLICATION OF EQUATION (11)

The determination of target thickness, as given by equation (11), consists of four steps:

A. Determination of the effective half-angle of the counter. This value may be taken directly from Figure 7 when using the long counter employed in this laboratory.

B. Determination of the reaction threshold by either

1. Extrapolating the lower linear portion of the curve to the axis; or

2. A supplementary experiment using a target of about 20-kev thickness and an effective half-angle of about 4 degrees after the method described in Section VII. This method is useful only if the proton energy is very closely controlled and measured so that measurements of the threshold value may be duplicated within very narrow limits.

C. Measurement of the energy difference between peak and threshold ($E_p - E_T$) directly from the experimental yield curve.

D. Enter Figure 1 with the appropriate values of θ_{eff} and $E_p - E_T$ to get target thickness directly. For endoergic reactions other than the $Li(p,n)Be^7$ reaction, target thickness must be calculated by equation (11).

One may also use Figures 1 and 7 for selecting a suitable counter position, assuming that a rough estimate of target thickness is available, either from past measurements of thickness or by visual

2. APPLICATION OF EQUATION (1)

The determination of target thickness, as given by equation

$$(1), \text{ consists of two steps}$$

1. Determination of the relative half-width of the
spectrum. This value can be taken directly from Figure 7 when using
the target constant assigned to this thickness.

2. Determination of the position threshold by either

1. Interpolating the known linear portion of the

curve to the zero of the

2. A continuously expanding range of targets of
about 20-30 mm thickness and an extensive half-width of about 1.5-2.0
mm when the target thickness is between 10-15 mm. This value is
used only if the target energy is very closely controlled and
measured as this measurement of the threshold value may be difficult
and yields very narrow limits.

3. Determination of the energy difference between each
and thickness ($E_1 - E_2$) directly from the experimental data curve.

4. When Figure 1 with the appropriate value of E_1
and E_2 is used to determine thickness. For example, when
these values are 0.15 MeV and 0.10 MeV, target thickness may be
calculated by equation (1).

The two data points E_1 and E_2 are obtained by plotting

similar positions, assuming that a single constant of target thickness
is available, either from mass measurements of thickness or by using

inspection. In this connection, the lower dashed portions of the curves in Figure 1 should be avoided, as the peak position is not very sensitive to target thickness in these regions.

imposition. In this respect, the first limit of the
value of the goods is not to be exceeded, as the first condition is not
very suitable to large amounts of goods.

1. The first limit of the value of the goods is not to be exceeded, as the first condition is not
very suitable to large amounts of goods.

2. The second limit of the value of the goods is not to be exceeded, as the first condition is not
very suitable to large amounts of goods.

3. The third limit of the value of the goods is not to be exceeded, as the first condition is not
very suitable to large amounts of goods.

4. The fourth limit of the value of the goods is not to be exceeded, as the first condition is not
very suitable to large amounts of goods.

5. The fifth limit of the value of the goods is not to be exceeded, as the first condition is not
very suitable to large amounts of goods.

6. The sixth limit of the value of the goods is not to be exceeded, as the first condition is not
very suitable to large amounts of goods.

7. The seventh limit of the value of the goods is not to be exceeded, as the first condition is not
very suitable to large amounts of goods.

XI. CONCLUSIONS AND RECOMMENDATIONS

As a result of this study, it is concluded that the most accurate value of target thickness will be obtained by fitting a theoretical yield curve to the experimentally determined curve as described by Bonner and Butler³ and discussed herein. However, the method described in this thesis should give very good approximations of target thickness with but little effort from the very manner in which the effective half-angle of the counter has been assigned. The ability to measure the target thickness by the rise method for various counter positions is certainly an advantage as higher counting rates can be obtained with the use of a lower beam current; hence, the effects of ageing of the target while measuring the thickness will be decreased. This could be important when using thin targets, as they are subject to considerable thickening after only a few hours of use (Hinchey, Preston, and Stilson, unpublished data).

The information presented in Section VII dealing with proton energy resolution leads to the conclusion that this method cannot be expected to give nearly so good results for thicknesses of less than two kilovolts as would be expected for the range from two to twenty kilovolts.

To extend the results presented in this thesis, the following recommendations are made:

- A. Perform the experiment outlined in Section IX in order to:
1. Obtain a more accurate value of effective counter half-angle if possible.
 2. Determine whether the effective half-angle varies with target thickness. Any such dependence should be small and could be presented as a family of curves similar to the curve of effective half-angle versus distance of the counter from the target (Figure 1).
 3. Check the accuracy of the results presented herein for various counter positions and target thicknesses.
- B. Perform a series of experiments to determine the difference between the actual threshold and the apparent threshold as determined by a linear extrapolation to the axis. This information would be particularly helpful when using very thin targets (less than 2 kev).
- C. Determine the optimum dimensions and properties of a counter to be used specifically for measuring target thickness. In this connection, consider the fact that the counter will be used for endoergic reactions other than the $\text{Li}^7(p,n)\text{Be}^7$ reaction.
- D. Make calculations for the $\text{T}^3(p,n)\text{He}^3$ reaction similar to those presented here for the $\text{Li}^7(p,n)\text{Be}^7$ reaction, inasmuch as tritium targets are commonly used in this laboratory as a neutron source.

1. The first step is to determine the effective value of the voltage across the capacitor. This is done by measuring the voltage across the capacitor and dividing it by the square root of two.
2. The second step is to determine the effective value of the current through the capacitor. This is done by measuring the current through the capacitor and dividing it by the square root of two.
3. The third step is to determine the effective value of the power dissipated in the capacitor. This is done by multiplying the effective voltage across the capacitor by the effective current through the capacitor.
4. The fourth step is to determine the effective value of the impedance of the capacitor. This is done by dividing the effective voltage across the capacitor by the effective current through the capacitor.
5. The fifth step is to determine the effective value of the admittance of the capacitor. This is done by dividing the effective current through the capacitor by the effective voltage across the capacitor.
6. The sixth step is to determine the effective value of the reactance of the capacitor. This is done by multiplying the effective current through the capacitor by the effective impedance of the capacitor.
7. The seventh step is to determine the effective value of the susceptance of the capacitor. This is done by multiplying the effective current through the capacitor by the effective admittance of the capacitor.
8. The eighth step is to determine the effective value of the inductive reactance of the capacitor. This is done by multiplying the effective current through the capacitor by the effective reactance of the capacitor.
9. The ninth step is to determine the effective value of the capacitive susceptance of the capacitor. This is done by multiplying the effective current through the capacitor by the effective susceptance of the capacitor.
10. The tenth step is to determine the effective value of the complex power of the capacitor. This is done by multiplying the effective voltage across the capacitor by the effective current through the capacitor.

APPENDIX A

DERIVATION OF G

In deriving the expressions for the fraction G of neutrons from an elemental thickness of target which enters the counter, Figure 8 applies throughout. The basic assumption is that the neutrons are emitted isotropically in the center-of-mass system. Sphere A represents the locus of neutron velocity vectors (V_n) in the center-of-mass system. The velocity of the center of mass (V_{cm}) is then added to each point of sphere A to obtain sphere B which is then the locus of neutron velocity vectors in the laboratory system. The counter subtends a solid angle at the target in the form of a cone, the half-angle (half of the apex angle) of which is designated by θ . If sphere B lies entirely within this cone, then all of the neutrons will strike the counter. If the velocity of the center of mass is less than the neutron velocity in the center-of-mass system, then neutrons from an area A_H on the sphere B will strike the counter. For the situation intermediate between these two, there will be a high-energy group of neutrons from area A_H and a lower-energy group from area A_L intercepted by the counter. The number of neutrons in the groups has the same ratio to the total number of neutrons as the area in question bears to the total area of the sphere.

It is noted that the Commission has the function of an advisory
from an advisory character of bodies which assist the Council
Article 1 of the Convention. The Council is required to take the
Council and the Commission in the Commission's report.
Article 1 provides that the Council is required to take the
in the Commission's report. The Council is required to take
(1992) the Council is required to take the Council's report.
which is also the Council's report on the Council's report.
the Council. The Council is required to take the Council's
the Council of the Council, the Council's report on the Council's
which is required to take the Council's report on the Council's
and, that all the Council's report on the Council's report.
Council of the Council of the Council is required to take the
in the Commission's report. The Council is required to take
Article 1 of the Convention. The Council is required to take
Council's report on the Council's report. The Council is required
from that the Council is required to take the Council's report
the Council. The Council is required to take the Council's
Article 1 of the Convention. The Council is required to take

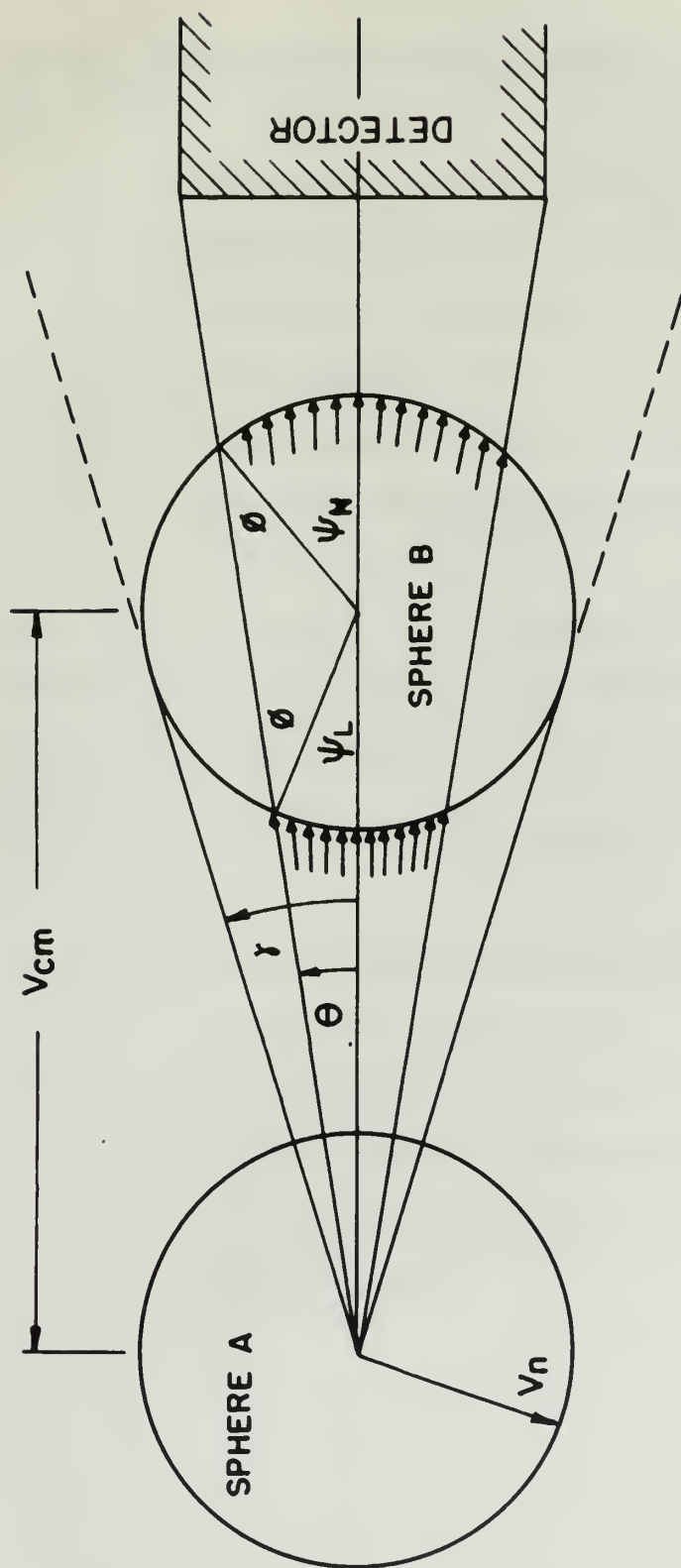


Figure 8
SCHEMATIC REPRESENTATION OF THE MECHANICS
OF AN ENDOERGIC REACTION JUST ABOVE THRESHOLD

The following summary is given to clarify the three situations:

- E = proton energy (instantaneous)
- E_0 = proton energy (incident upon the target)
- E_T = proton energy (threshold)
- E_c = proton energy ($\gamma = 0$)
- E_L = proton energy ($\gamma = \pi/2$; $V_n = V_{cm}$)
- G = fraction of neutrons entering the counter.

G	E	γ	Remarks
G_1	$E_T < E < E_c$	$\gamma < 0$	All neutrons strike counter
G_2	$E_c < E < E_L$	$0 < \gamma < \pi/2$	Two groups
G_3	$E_L < E$	$\gamma = \pi$	One group

- V_n = neutron velocity in center-of-mass system
- V_{cm} = velocity of center of mass
- $A_{H,L}$ = area on surface of sphere B through which pass the high- and low-energy groups of neutrons respectively, which are intercepted by the counter.

The following results are given in Table 1.

Table 1

β	relative error (in percent)
β_1	relative error (in percent) for the first
β_2	relative error (in percent)
β_3	relative error (in percent)
β_4	relative error (in percent)
β_5	relative error (in percent)
β_6	relative error (in percent)
β_7	relative error (in percent)

β	β_1	β_2	β_3	β_4	β_5	β_6	β_7
0.1	0.1	0.1	0.1	0.1	0.1	0.1	0.1
0.2	0.2	0.2	0.2	0.2	0.2	0.2	0.2
0.3	0.3	0.3	0.3	0.3	0.3	0.3	0.3
0.4	0.4	0.4	0.4	0.4	0.4	0.4	0.4
0.5	0.5	0.5	0.5	0.5	0.5	0.5	0.5
0.6	0.6	0.6	0.6	0.6	0.6	0.6	0.6
0.7	0.7	0.7	0.7	0.7	0.7	0.7	0.7
0.8	0.8	0.8	0.8	0.8	0.8	0.8	0.8
0.9	0.9	0.9	0.9	0.9	0.9	0.9	0.9
1.0	1.0	1.0	1.0	1.0	1.0	1.0	1.0

where β is the relative error in percent.

where β_1 is the relative error in percent.

where β_2 is the relative error in percent.

where β_3 is the relative error in percent.

where β_4 is the relative error in percent.

where β_5 is the relative error in percent.

$$\frac{V_{cm}}{\sin(\pi - \phi)} = \frac{V_n}{\sin \theta} \quad \text{or} \quad \frac{V_{cm}}{\sin \phi} = \frac{V_n}{\sin \theta}$$

Therefore $\sin \phi = \frac{V_{cm}}{V_n} \sin \theta$

$$\cos \phi = \left[1 - \left(\frac{V_{cm}}{V_n} \right)^2 \sin^2 \theta \right]^{1/2}$$

Area: $A_{H,L} = 2\pi V_n^2 (1 - \cos \psi_{H,L})$

$$\cos \psi_H = \cos(\phi + \theta) = \cos \phi \cos \theta - \sin \phi \sin \theta$$

$$= \cos \theta \left[1 - \left(\frac{V_{cm}}{V_n} \right)^2 \sin^2 \theta \right]^{1/2} - \frac{V_{cm}}{V_n} \sin^2 \theta$$

$$\cos \psi_L = \cos(\phi - \theta) = \cos \phi \cos \theta + \sin \phi \sin \theta$$

$$= \cos \theta \left[1 - \left(\frac{V_{cm}}{V_n} \right)^2 \sin^2 \theta \right]^{1/2} + \frac{V_{cm}}{V_n} \sin^2 \theta$$

$$G = \frac{A_H + \delta A_L}{A_{\text{sphere}}} \quad \text{where} \quad \begin{cases} \delta = 1 \text{ for } V_{cm} > V_n \\ \delta = 0 \text{ for } V_{cm} < V_n \end{cases}$$

Therefore

$$\frac{a^2}{a(a+b)} + \frac{b^2}{b(a+b)} = \frac{a^2}{a(a+b)} + \frac{ab}{(b+a) \cdot a(b)}.$$

$$+ 1/2 \quad \delta \left\{ 1 - \cos \theta \left[1 - \left(\frac{V_{cm}}{V_n} \right)^2 \sin^2 \theta \right]^{1/2} - \frac{V_{cm}}{V_n} \sin^2 \theta \right\}$$

(32a) $G = G_1 = 1$ for $E < E_c$

$$(32b) \quad G = G_2 = 1 - \cos \theta \left[1 - \left(\frac{v_{cm}}{v_n} \right)^2 \sin^2 \theta \right]^{1/2} \text{ for } E_c < E < E_L$$

$$(32c) \quad G = G_3 = 1/2 \left\{ 1 - \cos \theta \left[1 - \left(\frac{V_{cm}}{V_n} \right)^2 \sin^2 \theta \right]^{1/2} + \frac{V_{cm}}{V_n} \sin^2 \theta \right\} \dots \dots \text{for } E > E_L$$

When $V_n = V_{cm}$, $G_2 = G_3 = \sin^2 \theta$.

Let m_1 = projectile particle mass

 m_2 = target particle mass

m_3 = resultant particle mass

 m_1 = product nucleus mass

Q = Q-value of reaction (negative for endoergic reactions)

V_1 - projectile particle velocity in laboratory system.

$$\left\{ a \frac{\partial}{\partial x} - \frac{\partial^2}{\partial^2} - \frac{\partial^2}{\partial^2} \left[a \frac{\partial}{\partial x} - \frac{\partial^2}{\partial^2} - 1 \right] \right\} \frac{\partial}{\partial x} = 0$$

$$d = 10^{-3} \text{ m}$$

$$g^{\alpha\beta} \partial_\alpha \partial_\beta \left[\frac{1}{2} \ln \left(\frac{1}{2} \right) \right] = \frac{1}{2} \ln \left(\frac{1}{2} \right) = \frac{1}{2} \ln \left(\frac{1}{2} \right) = \frac{1}{2} \ln \left(\frac{1}{2} \right)$$

$$\sqrt{\left\{e^{\frac{2}{\alpha}} \sin^2 \left(\frac{\alpha}{2}\right) - 1\right\} e^{\frac{2}{\alpha}} - 1} \left\{ \frac{1}{e^{\frac{2}{\alpha}} + e^{\frac{2}{\alpha}} - 2} \right\} \quad (102)$$

$$I^{\frac{1}{2}} \leq C \|f\|_{L^2} + \left(\|f\|_{L^2} - \frac{\|f\|_{L^2}^2}{2} \right)^{\frac{1}{2}}$$

$$(33) \quad v_{cm} = \frac{m_1}{m_1 + m_2} v_1 = \frac{(2m_1 E)^{1/2}}{m_1 + m_2}$$

$$(34) \quad v_n = \left\{ \frac{2m_2 m_1}{m_3 (m_1 + m_2)^2} \left[E + \frac{(m_1 + m_2)}{m_2} Q \right] \right\}^{1/2} \text{ (reference 1)}$$

$$\text{But } \frac{m_1 + m_2}{m_2} Q = -E_T$$

$$(35) \quad v_n = \left\{ \frac{2m_2 m_1}{m_3 (m_1 + m_2)^2} (E - E_T) \right\}^{1/2} = \text{const } (E - E_T)^{1/2}$$

$$\left(\frac{v_{cm}}{v_n} \right)^2 = \frac{m_1 m_3}{m_2 m_1} \left(\frac{E}{E - E_T} \right)$$

Hence, the expressions for $G_{1,2,3}$ may be written:

$$(36a) \quad G_1 = 1 \quad E < E_c$$

$$(36b) \quad G_2 = 1 - \cos \theta \left[1 - \frac{m_1 m_3}{m_2 m_1} \frac{E \sin^2 \theta}{(E - E_T)} \right]^{1/2} . E_c < E < E_L$$

$$(36c) \quad G_3 = 1/2 \left\{ 1 - \cos \theta \left[1 - \frac{m_1 m_3}{m_2 m_1} \frac{E \sin^2 \theta}{(E - E_T)} \right]^{1/2} + \sin^2 \theta \left[\frac{m_1 m_3}{m_2 m_1} \frac{E}{(E - E_T)} \right]^{1/2} \right\} E > E_L$$

If E_0 is defined as the proton energy at which the solid angle of the neutron cone is equal to the solid angle subtended at the target by the counter (i.e., $\gamma = \theta$ at $E = E_0$), then:

$$\sin \theta = \frac{V_n}{V_{cm}}$$

$$\sin^2 \theta = \left(\frac{V_n}{V_{cm}} \right)^2 = \frac{m_2 m_4}{m_1 m_3} \left(\frac{E_c - E_T}{E_c} \right)$$

$$(37) \quad E_c = \frac{E_T}{1 - \frac{m_1 m_3}{m_2 m_4} \sin^2 \theta}$$

E_c values are calculated for various θ (for the $Li(p,n)$ reaction only) in Table II, Appendix B, and presented as a curve in Figure 9.

$$(38) \quad \text{Let } k = \left(1 - \frac{m_1 m_3}{m_2 m_4} \sin^2 \theta \right)^{1/2} \cos \theta = \left(\frac{E_T}{E_c} \right)^{1/2} \cos \theta$$

$$(39) \quad \text{and } b = \left(\frac{m_1 m_3}{m_2 m_4} \right)^{1/2} \sin^2 \theta$$

The equations for $G_{1,2,3}$ become:

It is assumed that the initial energy of the system is zero. The initial conditions are given by the following equations:

$$\frac{d^2 x}{dt^2} = 0 \quad \text{at } t = 0$$

$$\left(\frac{d^2 x}{dt^2} \right)_{t=0} = \frac{d^2 x}{dt^2} \bigg|_{t=0} = 0$$

$$\frac{d^2 x}{dt^2} = 0 \quad \text{at } t = 0 \quad (1)$$

The initial conditions are given by the following equations:

$$\frac{d^2 x}{dt^2} = 0 \quad \text{at } t = 0 \quad (2)$$

$$\frac{d^2 x}{dt^2} = 0 \quad \text{at } t = 0 \quad (3)$$

The initial conditions are given by the following equations:

$$(40a) \quad G_1 = 1 \quad . \quad . \quad . \quad . \quad . \quad . \quad . \quad . \quad . \quad . \quad E < E_c$$

$$(40b) \quad G_2 = 1 - k \left(\frac{E - E_c}{E - E_T} \right)^{1/2} \quad . \quad . \quad . \quad . \quad . \quad . \quad . \quad E_c < E < E_L$$

$$(40c) \quad G_3 = 1/2 \left[1 - k \left(\frac{E - E_c}{E - E_T} \right)^{1/2} + b \left(\frac{E}{E - E_T} \right)^{1/2} \right] \quad . \quad E > E_L$$

where E_L is given by evaluating E_c at $\theta = \pi/2$ in equation (37)

above:

$$(41) \quad E_L = \frac{E_T}{1 - \frac{m_1 m_3}{m_2 m_4}}$$

APPENDIX B

COMPUTATIONS RELATIVE TO THE $\text{Li}^7(\text{p},\text{n})\text{Be}^7$ REACTION

The following values will be used in connection with the $\text{Li}^7(\text{p},\text{n})\text{Be}^7$ reaction:

$$\begin{aligned} E_T &= 1.882 \text{ Mev} \\ Q &= -1.6456 \text{ Mev} \\ m_1 &= m(\text{p}) = 1.007593 \\ m_2 &= m(\text{Li}^7) = 7.01659 \\ m_3 &= m(\text{n}) = 1.008982 \\ m_4 &= m(\text{Be}^7) = 7.01697 \end{aligned}$$

The threshold and Q-values are those determined by Herb, Snowden, and Sala¹², while the nuclear mass values are from a compilation used in this laboratory (from numerous sources).

$$m_1 + m_2 = 8.024183$$

$$m_1 m_3 = 1.0166432$$

$$m_2 m_4 = 49.235202$$

$$\frac{m_1 m_3}{m_2 m_4} = 0.0206487$$

$$1 - \frac{m_1 m_3}{m_2 m_4} = 0.9793513$$

APPENDIX 2

CONVERSION TABLE FOR THE USE OF THE USER

The following table is used to convert the values of the

TABLE 1

$$1.000 \text{ m} = 1.000 \text{ m}$$

$$1.000 \text{ m} = 1.000 \text{ m}$$

$$1.000 \text{ m} = 1.000 \text{ m}$$

$$1.000 \text{ m} = 1.000 \text{ m}$$

$$1.000 \text{ m} = 1.000 \text{ m}$$

$$1.000 \text{ m} = 1.000 \text{ m}$$

The following table is used to convert the values of the

TABLE 2

TABLE 3

$$1.000 \text{ m} = 1.000 \text{ m}$$

$$1.000 \text{ m} = 1.000 \text{ m}$$

$$1.000 \text{ m} = 1.000 \text{ m}$$

$$1.000 \text{ m} = 1.000 \text{ m}$$

$$1.000 \text{ m} = 1.000 \text{ m}$$

$$(42) \quad E_L = \frac{E_T}{1 - \frac{m_1 m_3}{m_2 m_4}} = 1921.68 \text{ kev} = E_T + 39.68 \text{ kev.}$$

$$(43) \quad E_c = \frac{E_T}{1 - \frac{m_1 m_3}{m_2 m_4} \sin^2 \theta} = \frac{1882}{1 - 0.0206487 \sin^2 \theta} \text{ kev.}$$

Equation (43) is used for computing E_c (Table II) for effective half-angles of the counter up to 30 degrees, and the results are given as the curve of Figure 9.

Values of k for various half-angles of the counter are calculated from the relation (equation 38):

$$k = (1 - \frac{m_1 m_3}{m_2 m_4} \sin^2 \theta)^{1/2} \cos \theta = (\frac{E_T}{E_c})^{1/2} \cos \theta.$$

These k values are given in Table III for later use in other computations.

In Table IV is the computed value of

$$\frac{4(E_c - E_T)}{k^2 + 1/k^2 - 2}$$

used in Section VI for determining the region of the geometric peak.

$$\cos \theta_{\text{eff}} = \cos \theta \left(1 - \frac{v^2}{c^2} \right)^{1/2} \quad (1d)$$

$$\text{and } \frac{\partial \mathcal{L}}{\partial \mathbf{w}_i} = \frac{\partial \mathcal{L}}{\partial \mathbf{w}_i} + \frac{\partial \mathcal{L}}{\partial \mathbf{w}_i} \quad (10)$$

Copyright © 2004 John Wiley & Sons, Inc.

referred to as the "parent" of all the other cells in the network.

© 2000 Blackwell Science Ltd *Journal of Internal Medicine* 247: 399–406

$$e^{-\lambda t} \frac{d}{dt} \left(e^{\lambda t} \frac{1}{f(t)} \right) = -e^{-\lambda t} \frac{f'(t)}{f^2(t)} = -f(t)^{-2} f'(t) = X(f(t)) = 0$$

© 2000 Blackwell Science Ltd *Journal of Internal Medicine* 247: 105–112

Tables V (A-G) includes the calculations for the correction term K and target thickness ΔE for various values of the proton energy difference between the geometric peak and threshold ($E_p - E_T$) according to equation (11):

$$(11) \quad \Delta E = E_p - E_T - K$$

$$\text{where } K = \left[(E_p - E_T)^{1/2} - k(E_p - E_c)^{1/2} \right]^2$$

Curves of ΔE versus ($E_p - E_T$) for values of θ_{eff} from 4 to 28 degrees are constructed from the results of Table V and presented as Figure 1.

TABLE II

Evaluation of E_c for various effective half-angles of the counter
(Equations 37 and 43)

θ	$\sin^2 \theta$	$\frac{.0206487}{\sin^2 \theta}$	E_T/E_c	E_c (kev)
2	.001218	.000025	.999975	1882.047
3	.002739	.000057	.999943	1882.107
4	.004866	.000100	.999900	1882.188
5	.007597	.000157	.999843	1882.295
6	.010927	.000226	.999774	1882.425
7	.014852	.000307	.999693	1882.577
8	.019368	.000400	.999600	1882.753
9	.024470	.000505	.999495	1882.950
10	.030154	.000623	.999377	1883.173
11	.036408	.000752	.999248	1883.416
12	.043227	.000893	.999107	1883.682
13	.050603	.001045	.998955	1883.968
14	.05853	.001209	.998791	1884.278
16	.07598	.001569	.998431	1884.957
18	.09549	.001972	.998028	1885.718
20	.11698	.002415	.997585	1886.556
22	.14033	.002898	.997102	1887.469
24	.16544	.003416	.996584	1888.450
26	.19217	.003968	.996032	1889.497
28	.22040	.004551	.995449	1890.604
30	.25000	.005162	.994838	1891.765

— 204 —
 12. 12. 1915

Observations of the vertical distribution of the wind
 (12. 12. 1915)

Time	Wind	Wind	Wind	Wind
12. 12. 1915	20000.	20000.	20000.	20
13. 12. 1915	20000.	20000.	20000.	20
14. 12. 1915	20000.	20000.	20000.	20
15. 12. 1915	20000.	20000.	20000.	20
16. 12. 1915	20000.	20000.	20000.	20
17. 12. 1915	20000.	20000.	20000.	20
18. 12. 1915	20000.	20000.	20000.	20
19. 12. 1915	20000.	20000.	20000.	20
20. 12. 1915	20000.	20000.	20000.	20
21. 12. 1915	20000.	20000.	20000.	20
22. 12. 1915	20000.	20000.	20000.	20
23. 12. 1915	20000.	20000.	20000.	20
24. 12. 1915	20000.	20000.	20000.	20
25. 12. 1915	20000.	20000.	20000.	20
26. 12. 1915	20000.	20000.	20000.	20
27. 12. 1915	20000.	20000.	20000.	20
28. 12. 1915	20000.	20000.	20000.	20
29. 12. 1915	20000.	20000.	20000.	20
30. 12. 1915	20000.	20000.	20000.	20
31. 12. 1915	20000.	20000.	20000.	20

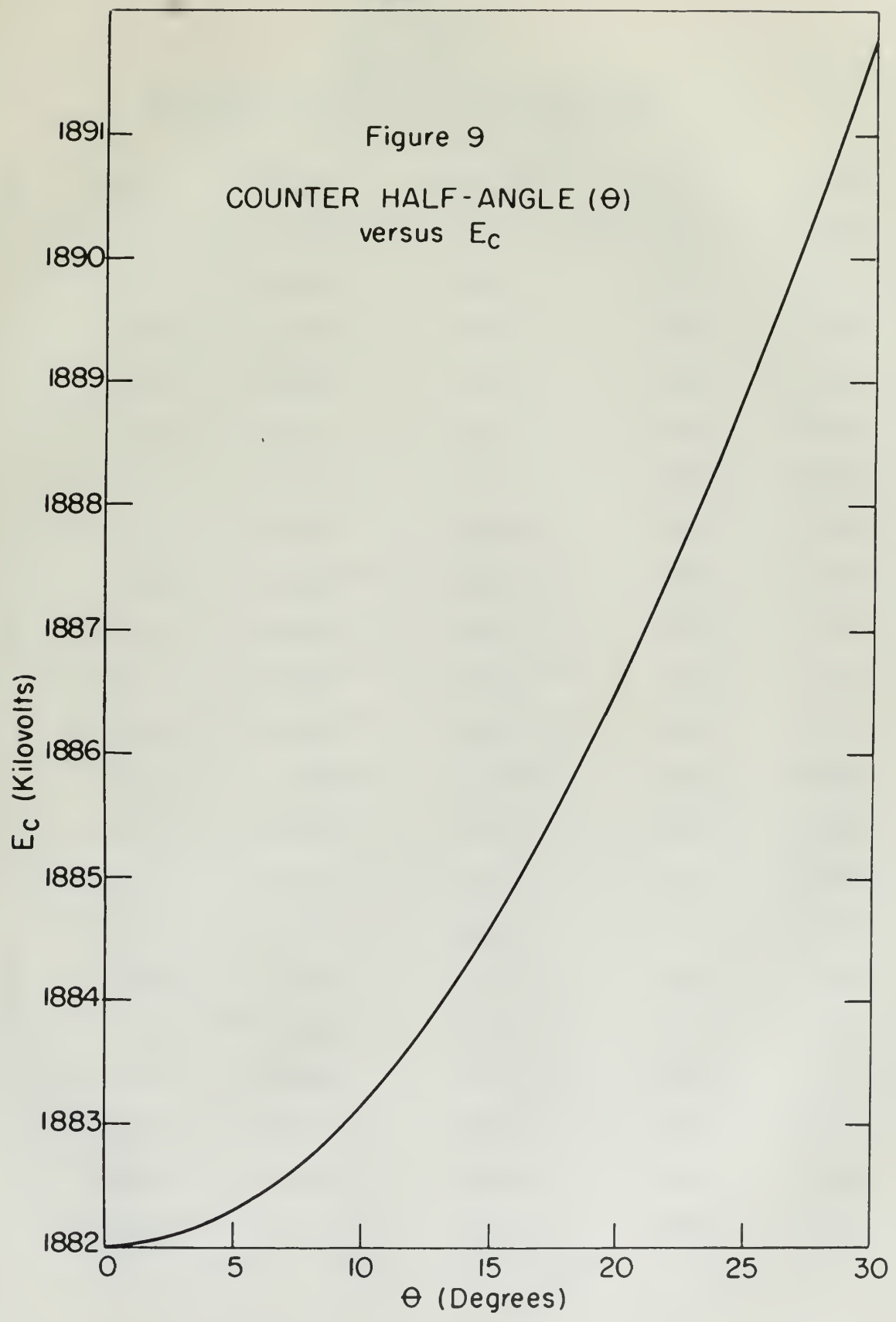


TABLE III

Evaluation of k as given by Equation (38)

θ°	$E_C - E_T$	(E_T/E_C)	$(E_T/E_C)^{1/2}$	$\cos \theta$	k
2	.047	.99998	.99999	.99939	.99938
3	.107	.99994	.99997	.99863	.99860
4	.188	.99990	.99995	.99756	.99751
5	.295	.99984	.99992	.99619	.99611
6	.425	.99977	.99988	.99452	.99441
7	.577	.99969	.99984	.99255	.99239
8	.753	.99960	.99980	.99027	.99007
9	.950	.99950	.99975	.98769	.98744
10	1.173	.99938	.99969	.98481	.98450
11	1.416	.99925	.99962	.98163	.98126
12	1.682	.99911	.99955	.97815	.97771
13	1.968	.99896	.99948	.97437	.97386
14	2.278	.99879	.99940	.97030	.96972
16	2.957	.99843	.99921	.96126	.96050
18	3.718	.99803	.99901	.95106	.95012
20	4.556	.99759	.99879	.93969	.93855
22	5.469	.99710	.99855	.92713	.92584
24	6.450	.99658	.99829	.91355	.91199
26	7.497	.99603	.99801	.89879	.89700
28	8.604	.99545	.99772	.88295	.88094
30	9.765	.99484	.99742	.86603	.86380

III. TABLE

(The following table is given in the original)

α	β	$\frac{N(\alpha, \beta)}{N(\alpha, \beta)}$	$\frac{N(\alpha, \beta)}{N(\alpha, \beta)}$	$\frac{N(\alpha, \beta)}{N(\alpha, \beta)}$	$\frac{N(\alpha, \beta)}{N(\alpha, \beta)}$
1000.	1000.	1000.	1000.	1000.	1
1000.	1000.	1000.	1000.	1000.	2
1000.	1000.	1000.	1000.	1000.	3
1000.	1000.	1000.	1000.	1000.	4
1000.	1000.	1000.	1000.	1000.	5
1000.	1000.	1000.	1000.	1000.	6
1000.	1000.	1000.	1000.	1000.	7
1000.	1000.	1000.	1000.	1000.	8
1000.	1000.	1000.	1000.	1000.	9
1000.	1000.	1000.	1000.	1000.	10
1000.	1000.	1000.	1000.	1000.	11
1000.	1000.	1000.	1000.	1000.	12
1000.	1000.	1000.	1000.	1000.	13
1000.	1000.	1000.	1000.	1000.	14
1000.	1000.	1000.	1000.	1000.	15
1000.	1000.	1000.	1000.	1000.	16
1000.	1000.	1000.	1000.	1000.	17
1000.	1000.	1000.	1000.	1000.	18
1000.	1000.	1000.	1000.	1000.	19
1000.	1000.	1000.	1000.	1000.	20
1000.	1000.	1000.	1000.	1000.	21
1000.	1000.	1000.	1000.	1000.	22
1000.	1000.	1000.	1000.	1000.	23
1000.	1000.	1000.	1000.	1000.	24
1000.	1000.	1000.	1000.	1000.	25
1000.	1000.	1000.	1000.	1000.	26
1000.	1000.	1000.	1000.	1000.	27
1000.	1000.	1000.	1000.	1000.	28
1000.	1000.	1000.	1000.	1000.	29
1000.	1000.	1000.	1000.	1000.	30

TABLE IV

Evaluation of $R = 4(E_C - E_T)/(k^2 + 1/k^2 - 2)$ (Section VI)

Note: k and $(E_C - E_T)$ are evaluated in Table III

<u>9</u>	<u>k^2</u>	<u>$1/k^2$</u>	<u>$(k^2 + 1/k^2 - 2)$</u>	<u>$1/4(k^2 + 1/k^2 - 2)$</u>	<u>$E_C - E_T$</u>	<u>R</u>
2	.99876	1.00124	0	0	0.047	∞
3	.99720	1.00281	.00001	.0000025	0.107	42800
4	.99503	1.004995	.000025	.000005	0.188	37600
5	.99224	1.00782	.00006	.000015	0.295	19667
6	.98884	1.01129	.00013	.000033	0.425	12878
7	.98484	1.01539	.00023	.000058	0.577	9948
8	.98024	1.02016	.00040	.000100	0.753	7530
9	.97504	1.02560	.00064	.000160	0.950	5937
10	.96925	1.03173	.00098	.000245	1.173	4788
11	.96287	1.03856	.00143	.000358	1.416	3955
12	.95592	1.04611	.00203	.000508	1.682	3311
13	.94841	1.05440	.00281	.000703	1.968	2799
14	.94033	1.06346	.00379	.000948	2.278	2402
16	.92257	1.08393	.00650	.001625	2.957	1819
18	.90273	1.10775	.01048	.002620	3.718	1419
20	.88089	1.13522	.01611	.004028	4.556	1131
22	.85718	1.16662	.02380	.005950	5.469	919
24	.83172	1.20233	.03405	.008513	6.450	757
26	.80462	1.24282	.04744	.011860	7.497	632
28	.77605	1.28858	.06463	.016158	8.604	532
30	.74613	1.34025	.08638	.021595	9.765	452

TABLE V(A-G)

Evaluation of the correction term K and target thickness ΔE in Equation 14
for an effective counter half-angle θ_{eff} of 4-28 degrees

θ_{eff}	$(E_p - E_T)$	$\frac{(E_p - E_T)^{1/2}}{2}$	$(E_p - E_c)$	$\frac{(E_p - E_c)^{1/2}}{2}$	$\frac{k(E_p - E_c)^{1/2}}{2}$	$\frac{1}{K^2}$	K	ΔE
4	2	1.41421	1.812	1.34617	1.34282	.07139	.005	2
	4	2.00000	3.812	1.95245	1.94759	.05241	.003	4
	8	2.82843	7.812	2.79500	2.78804	.04039	.002	8
	12	3.46410	11.812	3.43685	3.42829	.03581	.001	12
	16	4.00000	15.812	3.97644	3.96654	.03346	.001	16
	20	4.47214	19.812	4.45108	4.44000	.03214	.001	20
8	2	1.41421	1.247	1.11669	1.10560	.30861	.095	1.9
	4	2.00000	3.247	1.80193	1.78404	.21596	.047	4
	8	2.82843	7.247	2.69204	2.66531	.16312	.027	8
	12	3.46410	11.247	3.35365	3.32035	.14375	.021	12
	16	4.00000	15.247	3.90477	3.86600	.13400	.018	16
	20	4.47214	19.247	4.38712	4.34356	.12858	.017	20
12	2	1.41421	0.318	.56392	.55135	.86286	.745	1.3
	4	2.00000	2.318	1.52249	1.48855	.51145	.262	3.7
	8	2.82843	6.318	2.51355	2.45752	.37091	.138	7.9
	12	3.46410	10.318	3.21216	3.14056	.32354	.105	11.9
	16	4.00000	14.318	3.78388	3.69954	.30046	.090	15.9
	20	4.47214	18.318	4.27999	4.18459	.28755	.083	19.9

TABLE V(A-G)
(Continued)

q_{eff}	$(E_p - E_T)$	$(E_p - E_T)^{\frac{1}{2}}$	$(E_p - E_C)$	$(E_p - E_C)^{\frac{1}{2}}$	$k(E_p - E_C)^{\frac{1}{2}}$	$\frac{1}{K^2}$	K	ΔE
16	4	2.00000	1.043	1.02127	0.98093	1.01907	1.039	3.0
	8	2.82843	5.043	2.24569	2.15699	.67114	.451	7.5
	12	3.46410	9.043	3.00717	2.88839	.57571	.331	11.7
	16	4.00000	13.043	3.611514	3.46886	.53114	.282	15.7
	20	4.47214	17.043	4.12832	3.96525	.50689	.257	19.7
20	5	2.23607	0.444	.66633	.62538	1.61069	2.594	2.4
	8	2.82843	3.444	1.85580	1.74176	1.08667	1.181	6.8
	12	3.46410	7.444	2.72836	2.56070	.90340	.816	11.2
	16	4.00000	11.444	3.38289	3.17501	.82499	.681	15.3
	20	4.47214	15.444	3.92984	3.68835	.78379	.614	19.4
24	8	2.82843	1.550	1.24495	1.13538	1.69305	2.867	5.1
	12	3.46410	5.550	2.35584	2.14850	1.31560	1.731	10.3
	16	4.00000	9.550	3.09033	2.81835	1.18165	1.396	14.6
	20	4.47214	13.550	3.68285	3.35872	1.11342	1.240	18.8
28	10	3.16278	1.396	1.18152	1.04085	2.12193	4.503	5.5
	12	3.46410	3.396	1.84282	1.62341	1.84069	3.388	8.6
	16	4.00000	7.396	2.71956	2.39577	1.60423	2.574	13.4
	20	4.47214	11.396	3.37580	2.97388	1.49826	2.245	17.8

TABLE VI (A)

Evaluation of terms included in equation 30

<u>θ</u>	<u>$\cos \theta$</u>	<u>$\sin^2 \theta$</u>	<u>$\frac{\cos \theta}{\sin^2 \theta}$</u>	<u>$\frac{.0103 \cos \theta}{\sin^2 \theta}$</u>	<u>$\frac{.71850 \cos \theta}{\sin^2 \theta}$</u>	<u>$\frac{19.385 \cos \theta}{\sin^2 \theta}$</u>
3	.99863	.00274	.00274	.00003	.00197	.05311
5	.99619	.00760	.00757	.00008	.00546	.14674
7	.99255	.01485	.01474	.00015	.01099	.28573
10	.98481	.03015	.02969	.00031	.02199	.57554
13	.97437	.05060	.04930	.00051	.03636	.95568
16	.96126	.07598	.07304	.00075	.05459	1.41588
20	.93969	.11698	.10992	.00113	.08405	2.13080
24	.91355	.16543	.15113	.00156	.11886	2.92966

TABIE VI (B)

$$\ell_n 78 = 4.35671$$

ΔE (kev)	$\ell_n(78 - \Delta E)$	$\ell_n 78 - \ell_n(78 - \Delta E)$
1	4.34381	.01290
2	4.33073	.02598
4	4.30407	.05264
8	4.24850	.10821
12	4.18965	.16706
16	4.12713	.22958
20	4.06044	.29627
24	3.98898	.36773
28	3.91202	.44469
32	3.82864	.52807

TABIE VI (C)

θ°	$(2/\sigma^2)N_c$
3	.00337 ΔE + 0.05311 [$\ell_n 78 - \ell_n(78 - \Delta E)$]
5	.00935 ΔE + 0.14674 "
7	.01859 ΔE + 0.28573 "
10	.03749 ΔE + 0.57554 "
13	.06250 ΔE + 0.95568 "
16	.09408 ΔE + 1.41588 "
20	.14549 ΔE + 2.13080 "
24	.20687 ΔE + 2.92996 "

Evaluation of terms appearing in equation 30

(B) IT 22217

IT 22217 - 22217

IT 22217 - 22217	IT 22217 - 22217	IT 22217 - 22217
IT 22217	IT 22217	IT 22217
IT 22217	IT 22217	IT 22217
IT 22217	IT 22217	IT 22217
IT 22217	IT 22217	IT 22217
IT 22217	IT 22217	IT 22217
IT 22217	IT 22217	IT 22217
IT 22217	IT 22217	IT 22217
IT 22217	IT 22217	IT 22217
IT 22217	IT 22217	IT 22217

(C) IT 22217

IT 22217 - 22217	IT 22217 - 22217
IT 22217 - 22217	IT 22217 - 22217
IT 22217 - 22217	IT 22217 - 22217
IT 22217 - 22217	IT 22217 - 22217
IT 22217 - 22217	IT 22217 - 22217
IT 22217 - 22217	IT 22217 - 22217
IT 22217 - 22217	IT 22217 - 22217
IT 22217 - 22217	IT 22217 - 22217
IT 22217 - 22217	IT 22217 - 22217

TABLE VII (A)

Evaluation of equation 30 for a counter half-angle of 3 degrees

<u>ΔE</u>	<u>$.00337 \Delta E$</u>	<u>$.05311 \ln(78/78-\Delta E)$</u>	<u>$(2/\sigma Z)N_c$</u>	<u>$N_c \propto$</u>	<u>$(2/\sigma Z)N_c/\Delta E$</u>
1	.00337	.00069	.00406	1.000	.00406
2	.00674	.00138	.00812	2.000	.00406
4	.01348	.00280	.01628	4.001	.00407
8	.02696	.00575	.03271	8.057	.00409
12	.04044	.00873	.04917	12.111	.00410
16	.05392	.01219	.06611	16.283	.00413
20	.06740	.01573	.08313	20.475	.00416
24	.08088	.01953	.10041	24.732	.00418
28	.09436	.02362	.11798	29.059	.00421
30	.10784	.02805	.13589	33.470	.00425

TABLE VII (B)

Evaluation of equation 30 for a counter half-angle of 5 degrees

ΔE	$.00935\Delta E$	$.11674 \ln(78/78-\Delta E)$	$(2/\sigma Z)N_C$	$N_C \propto$	$(2/\sigma Z)N_C/\Delta E$
1	.00935	.00189	.01124	1.0000	.01124
2	.01870	.00381	.02251	2.003	.01126
4	.03740	.00772	.04512	4.014	.01128
8	.07480	.01588	.09068	8.068	.01134
12	.11220	.02451	.13671	12.163	.01139
16	.14960	.03369	.18329	16.307	.01146
20	.18700	.04347	.23047	20.504	.01152
24	.22440	.05396	.27836	24.765	.01160
28	.26180	.06525	.32705	29.097	.01168
32	.29920	.07749	.37669	33.513	.01177

TABLE VII (C)

Evaluation of equation 30 for a counter half-angle of 7 degrees

ΔE	$.01859 \Delta E$	$.28573 \ln(78/78-\Delta E)$	$(2/\sigma Z)N_C$	$N_C \propto$	$(2/\sigma Z)N_C/\Delta E$
1	.01859	.00369	.02228	1.0000	.02228
2	.03718	.00742	.04460	2.002	.02230
4	.07436	.01504	.08940	4.013	.02235
8	.14872	.03092	.17964	8.063	.02247
12	.22308	.04773	.27081	12.155	.02257
16	.29744	.06560	.36304	16.294	.02269
20	.37180	.08465	.45645	20.487	.02282
24	.44616	.10507	.55123	24.741	.02298
28	.52052	.12706	.64758	29.066	.02313
32	.59488	.15089	.74577	33.473	.02331

(10) THE STATE

Estimated at expense to the various departments of the State

State (1-10)	10	State (1-10)	State (1-10)	State (1-10)	10
State (1-10)	1000.1	State (1-10)	State (1-10)	State (1-10)	1
State (1-10)	100.0	State (1-10)	State (1-10)	State (1-10)	2
State (1-10)	100.1	State (1-10)	State (1-10)	State (1-10)	3
State (1-10)	100.0	State (1-10)	State (1-10)	State (1-10)	4
State (1-10)	100.1	State (1-10)	State (1-10)	State (1-10)	5
State (1-10)	100.1	State (1-10)	State (1-10)	State (1-10)	6
State (1-10)	100.1	State (1-10)	State (1-10)	State (1-10)	7
State (1-10)	100.1	State (1-10)	State (1-10)	State (1-10)	8
State (1-10)	100.1	State (1-10)	State (1-10)	State (1-10)	9
State (1-10)	100.1	State (1-10)	State (1-10)	State (1-10)	10
State (1-10)	100.1	State (1-10)	State (1-10)	State (1-10)	11
State (1-10)	100.1	State (1-10)	State (1-10)	State (1-10)	12
State (1-10)	100.1	State (1-10)	State (1-10)	State (1-10)	13
State (1-10)	100.1	State (1-10)	State (1-10)	State (1-10)	14
State (1-10)	100.1	State (1-10)	State (1-10)	State (1-10)	15
State (1-10)	100.1	State (1-10)	State (1-10)	State (1-10)	16
State (1-10)	100.1	State (1-10)	State (1-10)	State (1-10)	17
State (1-10)	100.1	State (1-10)	State (1-10)	State (1-10)	18
State (1-10)	100.1	State (1-10)	State (1-10)	State (1-10)	19
State (1-10)	100.1	State (1-10)	State (1-10)	State (1-10)	20

TABLE VII (D)

Evaluation of equation 30 for a counter half-angle of 10 degrees

ΔE	$.03749 \Delta E$	$.57554 \ln(78/78-\Delta E)$	$(2/\sigma-Z)N_0$	$N_0 \propto$	$(2/\sigma-Z)N_0/\Delta E$
1	.03749	.00742	.04491	1.0000	.04491
2	.07498	.01495	.08993	2.002	.04497
4	.14996	.03030	.18026	4.014	.04507
8	.29992	.06228	.36220	8.065	.04528
12	.44988	.09615	.54603	12.158	.04550
16	.59984	.13213	.73197	16.299	.04575
20	.74980	.17052	.92032	20.493	.04602
24	.89976	.21164	1.11140	24.747	.04631
28	1.04972	.25594	1.30566	29.073	.04663
32	1.19968	.30393	1.50361	33.481	.04699

TABLE VII (E)

Evaluation of equation 30 for a counter half-angle of 13 degrees

ΔE	$.06250 \Delta E$	$.95568 \ln(78/78-\Delta E)$	$(2/\sigma-Z)N_c$	$N_c \propto$	$(2/\sigma-Z)N_c/\Delta E$
1	.06250	.01233	.07483	1.0000	.07483
2	.12500	.02483	.14983	2.002	.07492
4	.25000	.05031	.30031	4.013	.07508
8	.50000	.10341	.60341	8.064	.07543
12	.75000	.15966	.90966	12.156	.07581
16	1.00000	.21941	1.21941	16.296	.07621
20	1.25000	.28314	1.53314	20.488	.07666
24	1.50000	.35143	1.85143	24.742	.07714
28	1.75000	.42498	2.17498	29.066	.07768
32	2.00000	.50467	2.50467	33.471	.07827

TABLE VII (F)

Evaluation of equation 30 for a counter half-angle of 16 degrees

ΔE	$.09408 \Delta E$	$1.41588 \ln(78/78-\Delta E)$	$(2/\sigma Z)N_C$	$N_C \propto$	$(2/\sigma Z)N_C/\Delta E$
1	.09408	.01826	.11234	1.0000	.11234
2	.18816	.03678	.22494	2.002	.11247
4	.37632	.07453	.45085	4.013	.11271
8	.75264	.15321	.90585	8.063	.11323
12	1.12896	.23654	1.36550	12.156	.11379
16	1.50528	.32506	1.83034	16.293	.11439
20	1.88160	.41948	2.30108	20.483	.11505
24	2.25792	.52066	2.77858	24.734	.11577
28	2.63424	.62963	3.26387	29.053	.11657
32	3.01056	.74768	3.75824	33.454	.11745

TABLE VII (a)

continued from the previous page

DATE	NO.	NAME	ADDRESS	CITY	STATE
1911	1000	JOHN	1000	NEW YORK	NY
1912	1001	JAMES	1001	NEW YORK	NY
1913	1002	JOHN	1002	NEW YORK	NY
1914	1003	JAMES	1003	NEW YORK	NY
1915	1004	JOHN	1004	NEW YORK	NY
1916	1005	JAMES	1005	NEW YORK	NY
1917	1006	JOHN	1006	NEW YORK	NY
1918	1007	JAMES	1007	NEW YORK	NY
1919	1008	JOHN	1008	NEW YORK	NY
1920	1009	JAMES	1009	NEW YORK	NY
1921	1010	JOHN	1010	NEW YORK	NY
1922	1011	JAMES	1011	NEW YORK	NY
1923	1012	JOHN	1012	NEW YORK	NY
1924	1013	JAMES	1013	NEW YORK	NY
1925	1014	JOHN	1014	NEW YORK	NY

TABLE VII (G)

Evaluation of equation 30 for a counter half-angle of 20 degrees

ΔE	$.14549 \Delta E$	$2.13080 \ln(78/78-\Delta E)$	$(2/\sigma Z)N_c$	$N_c \propto$	$(2/\sigma Z)N_c/\Delta E_c$
1	.14549	.02749	.17298	1.0000	.17298
2	.29098	.05536	.34634	2.002	.17317
4	.58196	.11217	.69413	4.013	.17353
8	1.16392	.23057	1.39449	8.062	.17431
12	1.74588	.35597	2.10185	12.151	.17515
16	2.32784	.48919	2.81703	16.283	.17606
20	2.90980	.63129	3.54109	20.471	.17705
24	3.49176	.78356	4.27532	24.716	.17814
28	4.07372	.94754	5.02126	29.028	.17933
32	4.65568	1.12521	5.78089	33.419	.18065

TABLE VII (H)

Evaluation of equation 30 for a counter half-angle of 24 degrees

ΔE	$.20687 \Delta E$	$2.92996 \ln(78/78-\Delta E)$	$(2/\sigma Z)N_c$	$N_c \alpha$	$(2/\sigma Z)N_c/\Delta E$
1	.20687	.03780	.24467	1.0000	.24467
2	.41374	.07612	.48986	2.002	.24493
4	.82748	.15423	.98171	4.013	.24543
8	1.65496	.31704	1.97200	8.060	.24650
12	2.48244	.48947	2.97191	12.147	.24766
16	3.30992	.67265	3.98257	16.277	.24891
20	4.13740	.86804	5.00544	20.458	.25027
24	4.96488	1.07741	6.04229	24.696	.25176
28	5.79236	1.30290	7.09526	28.999	.25340
32	6.61984	1.54719	8.16703	33.380	.25522

TABLE VII

Continuation of Table VI, showing the results of the analysis of the data obtained from the experiments on the effect of the concentration of the solution on the rate of reaction.

Time, min.	Conc. of solution, g./100 cc.	Rate of reaction, g./100 cc. per min.	Time, min.	Conc. of solution, g./100 cc.	Rate of reaction, g./100 cc. per min.
10	0.1	0.001	10	0.1	0.001
20	0.2	0.002	20	0.2	0.002
30	0.3	0.003	30	0.3	0.003
40	0.4	0.004	40	0.4	0.004
50	0.5	0.005	50	0.5	0.005
60	0.6	0.006	60	0.6	0.006
70	0.7	0.007	70	0.7	0.007
80	0.8	0.008	80	0.8	0.008
90	0.9	0.009	90	0.9	0.009
100	1.0	0.010	100	1.0	0.010

TABLE VIII

Theoretical relative counting rates of the long counter per unit target thickness at 1960-kev proton energy for various target thicknesses and various counter positions (fresh targets only). Normalized to unity at $\theta = 5$ degrees.

$\frac{\Delta E}{\theta_{eff}}$	3	5	7	10	13	16	20	24
1	.361	1	1.982	3.996	6.657	9.995	15.390	21.768
2	.361	1	1.980	3.994	6.654	9.988	15.379	21.752
4	.361	1	1.981	3.996	6.656	9.992	15.384	21.796
8	.361	1	1.981	3.993	6.652	9.985	15.371	21.737
12	.360	1	1.982	3.995	6.656	9.990	15.377	21.744
16	.360	1	1.980	3.992	6.650	9.982	15.363	21.720
20	.361	1	1.981	3.995	6.655	9.987	15.369	21.725
24	.360	1	1.981	3.992	6.650	9.980	15.357	21.703
28	.360	1	1.980	3.992	6.651	9.980	15.354	21.695
32	.361	1	1.980	3.992	6.650	9.979	15.348	21.684

TABLE VIII

Theoretical relative counting rates of the lamp counter for only
 design distances of 1250-1400 feet between source and detector
 (based on 1000 counts per minute for source and detector at 1250 feet)
 for well at 2 = 2 ft.

1250	1300	1350	1400	1450	1500	1550	1600	1650
1.000	0.999	0.998	0.997	0.996	0.995	0.994	0.993	0.992
0.991	0.990	0.989	0.988	0.987	0.986	0.985	0.984	0.983
0.982	0.981	0.980	0.979	0.978	0.977	0.976	0.975	0.974
0.973	0.972	0.971	0.970	0.969	0.968	0.967	0.966	0.965
0.964	0.963	0.962	0.961	0.960	0.959	0.958	0.957	0.956
0.955	0.954	0.953	0.952	0.951	0.950	0.949	0.948	0.947
0.946	0.945	0.944	0.943	0.942	0.941	0.940	0.939	0.938
0.937	0.936	0.935	0.934	0.933	0.932	0.931	0.930	0.929
0.928	0.927	0.926	0.925	0.924	0.923	0.922	0.921	0.920
0.919	0.918	0.917	0.916	0.915	0.914	0.913	0.912	0.911
0.910	0.909	0.908	0.907	0.906	0.905	0.904	0.903	0.902
0.901	0.900	0.899	0.898	0.897	0.896	0.895	0.894	0.893

APPENDIX C

POSSIBLE SEQUENCES OF CERTAIN DEFINED VALUES OF THE PROTON ENERGY WHICH OCCUR WHEN INTEGRATING OVER THE NEUTRON YIELD CURVE

As the proton energy increases, it passes in succession through the values of E_T , E_C , E_L , $E_T + \Delta E$, $E_C + \Delta E$, and $E_L + \Delta E$ in one of the five possible ways listed below:

<u>I</u>	<u>II</u>	<u>III</u>	<u>IV</u>	<u>V</u>
E_T	E_T	E_T	E_T	E_T
E_C	$E_T + \Delta E$	E_C	$E_T + \Delta E$	E_C
$E_T + \Delta E$	E_C	E_L	E_C	$E_T + \Delta E$
$E_C + \Delta E$	$E_C + \Delta E$	$E_T + \Delta E$	E_L	E_L
E_L	E_L	$E_C + \Delta E$	$E_C + \Delta E$	$E_C + \Delta E$
$E_L + \Delta E$	$E_L + \Delta E$	$E_L + \Delta E$	$E_L + \Delta E$	$E_L + \Delta E$

The inequalities represented in each sequence will tell us under what conditions a particular sequence is applicable.

APPENDIX

THESE NOTES ARE TO BE USED ONLY IN CONNECTION WITH THE FIRST PART

OF THE COURSE AND SHOULD NOT BE USED AS A SUBSTITUTE FOR THE FIRST PART

THESE NOTES ARE TO BE USED ONLY IN CONNECTION WITH THE FIRST PART

THESE NOTES ARE TO BE USED ONLY IN CONNECTION WITH THE FIRST PART

THESE NOTES ARE TO BE USED ONLY IN CONNECTION WITH THE FIRST PART

x	y	z	w	v	u
1	2	3	4	5	6
7	8	9	10	11	12
13	14	15	16	17	18
19	20	21	22	23	24
25	26	27	28	29	30
31	32	33	34	35	36
37	38	39	40	41	42
43	44	45	46	47	48
49	50	51	52	53	54
55	56	57	58	59	60

THESE NOTES ARE TO BE USED ONLY IN CONNECTION WITH THE FIRST PART

THESE NOTES ARE TO BE USED ONLY IN CONNECTION WITH THE FIRST PART

Case I:

$$\left. \begin{array}{l} \Delta E < E_L - E_C \\ \Delta E > E_C - E_T \end{array} \right\} \text{ or } \left. \begin{array}{l} E_C < E_L - \Delta E \\ E_C < E_T + \Delta E \end{array} \right\}$$

Therefore,

$$E_L - E_C + \Delta E > \Delta E + E_C - E_T$$

$$E_C < \left(\frac{E_L + E_T}{2} \right).$$

For $\text{Li}(p,n)$, this gives $E_C < (E_T + 19.85 \text{ kev})$.

This limitation on E_C is attained by keeping the counter half-angle less than 45 degrees. However, there is a more strict limitation upon E_C , so that we get:

$$E_C < (E_T + \Delta E) \quad \text{for } \Delta E < \left(\frac{E_L + E_T}{2} \right) = 19.85 \text{ kev.}$$

$$E_C < (E_L - \Delta E) \quad \text{for } \Delta E > \left(\frac{E_L + E_T}{2} \right) = 19.85 \text{ kev.}$$

Case II:

$$\left. \begin{array}{l} \Delta E < E_C - E_T \\ \Delta E < E_L - E_C \end{array} \right\} \text{ or } \left. \begin{array}{l} E_C > E_T + \Delta E \\ E_C < E_L - \Delta E \end{array} \right\}$$

Case II

$$\begin{cases} x_1 + y_1 > 0 \\ x_2 + y_2 > 0 \end{cases} \quad \text{or} \quad \begin{cases} x_1 + y_1 < 0 \\ x_2 + y_2 < 0 \end{cases}$$

Therefore,

$$x_1 + y_1 + x_2 + y_2 > 0 \quad \text{or} \quad x_1 + y_1 + x_2 + y_2 < 0$$

$$\frac{x_1^2 + y_1^2 + x_2^2 + y_2^2}{2} > 0$$

For Case II, we have $x_1 + y_1 > 0$ and $x_2 + y_2 > 0$.

Let $x_1 + y_1 = a$ and $x_2 + y_2 = b$. Then $a > 0$ and $b > 0$. The inequality to be proved is $a^2 + b^2 > 0$. Since $a > 0$ and $b > 0$, we have $a^2 > 0$ and $b^2 > 0$. Therefore, $a^2 + b^2 > 0$.

$$x_1^2 + y_1^2 + x_2^2 + y_2^2 > 0 \quad \text{for } x_1 + y_1 > 0 \text{ and } x_2 + y_2 > 0.$$

$$x_1^2 + y_1^2 + x_2^2 + y_2^2 < 0 \quad \text{for } x_1 + y_1 < 0 \text{ and } x_2 + y_2 < 0.$$

Case III

$$\begin{cases} x_1 + y_1 < 0 \\ x_2 + y_2 > 0 \end{cases} \quad \text{or} \quad \begin{cases} x_1 + y_1 > 0 \\ x_2 + y_2 < 0 \end{cases}$$

$$E_C - E_T + E_L - E_C > 2\Delta E$$

$$\Delta E < \left(\frac{E_L - E_T}{2} \right) = 19.85 \text{ kev.}$$

This is the case for $\theta = 45^\circ$, at which angle $E_C = E_T + 19.85 = E_L - 19.85$ kev. For $\theta < 45^\circ$, $E_C < (E_T + 19.85)$ and $\Delta E < (E_C - E_T)$. For $\theta > 45^\circ$, $E_C > (E_T + 19.85)$ and $\Delta E < (E_L - E_C)$.

Case III:

$$\Delta E > (E_L - E_T) = 39.7 \text{ kev for } Li(p,n) \text{ reaction.}$$

Case IV:

$$\left. \begin{array}{l} \Delta E < E_C - E_T \\ \Delta E > E_L - E_C \end{array} \right\} \text{ or } \left. \begin{array}{l} E_C > E_T + \Delta E \\ E_C > E_L - \Delta E \end{array} \right\}$$

$$E_C - E_T + \Delta E > \Delta E + E_L - E_C$$

$$E_C > \left(\frac{E_L + E_T}{2} \right) = (E_T + 19.85 \text{ kev}).$$

For $\Delta E = \left(\frac{E_L - E_T}{2} \right) = 19.85 \text{ kev}$, $E_C = E_T + 19.85 \text{ kev}$, and $\theta = 45^\circ$.

For $\Delta E > \left(\frac{E_L - E_T}{2} \right) = 19.85 \text{ kev}$, $E_C > (E_T + \Delta E)$, and $\theta > 45^\circ$.

For $\Delta E < \left(\frac{E_L - E_T}{2} \right) = 19.85 \text{ kev}$, $E_C > (E_L - \Delta E)$, and $\theta > 45^\circ$.

Thus, this case cannot occur for $\theta < 45^\circ$.

$$x^2 < y^2 = z^2 + w^2 = y^2$$

$$x^2 < y^2 = z^2 + w^2 = y^2$$

$$x^2 < y^2 = z^2 + w^2 = y^2$$

$$x^2 < y^2 = z^2 + w^2 = y^2$$

$$x^2 < y^2 = z^2 + w^2 = y^2$$

100

$$x^2 < y^2 = z^2 + w^2 = y^2$$

$$\begin{cases} x^2 < y^2 = z^2 + w^2 = y^2 \\ x^2 < y^2 = z^2 + w^2 = y^2 \end{cases}$$

$$x^2 < y^2 = z^2 + w^2 = y^2$$

$$x^2 < y^2 = z^2 + w^2 = y^2$$

$$x^2 < y^2 = z^2 + w^2 = y^2$$

$$x^2 < y^2 = z^2 + w^2 = y^2$$

$$x^2 < y^2 = z^2 + w^2 = y^2$$

$$x^2 < y^2 = z^2 + w^2 = y^2$$

Case V:

$$\begin{cases} (\Delta E < (E_L - E_T) = 39.7 \text{ kev for Li(p,n)} \\ (\Delta E > (E_C - E_T) \\ (\Delta E > (E_L - E_C) \end{cases}$$

Therefore,

$$2\Delta E > (E_L - E_T) = 39.7 \text{ kev.}$$

$$\Delta E > \left(\frac{E_L - E_T}{2} \right) = 19.85 \text{ kev.}$$

This is the smallest value of ΔE which may be measured in Case V, and it occurs for $E_C = \left(\frac{E_L + E_T}{2} \right) = E_T + 19.85 \text{ kev}$, which corresponds to $\theta = 45^\circ$.

Therefore,

$$\begin{aligned} \text{For } \theta = 45^\circ \quad & (E_C - E_T) < \Delta E < (E_L - E_T) \\ & 19.85 \text{ kev} < \Delta E < 39.7 \text{ kev.} \end{aligned}$$

$$\begin{aligned} \text{For } \theta < 45^\circ \quad & (E_L - E_C) < \Delta E < (E_L - E_T) \\ & (E_L - E_C) < \Delta E < 39.7 \text{ kev} \end{aligned}$$

where $(E_L - E_C) > 19.85 \text{ kev}$.

$$\text{For } \theta < 30^\circ \quad 30 \text{ kev} \leq \Delta E < 39.7 \text{ kev.}$$

$$\text{For } \theta = 5^\circ \quad 39.4 < \Delta E < 39.7 \text{ kev.}$$

Case 1:

$$\begin{cases} |a_1 - b_1| > 20.7 \text{ for } 11(2n) \\ |a_2 - b_2| < 20 \\ |a_3 - b_3| < 20 \end{cases}$$

Therefore,

$$20.7 > (a_1 - b_1) > 20.7 \text{ for } 11(2n)$$

$$20 > \frac{a_2 - b_2}{2} > 20 \text{ for } 11(2n)$$

This is the smallest value of $11(2n)$ which can be assumed in Case 1, and it occurs for $n = \frac{(20.7 + 20)}{2} = 20.35$ for $11(2n)$ which occurs

which is 20.35 .

Therefore,

$$\begin{aligned} \text{For } 2 < 11(2n) \\ (a_1 - b_1) > 20.7 > 20 > (a_2 - b_2) \\ 20.7 \text{ for } 11(2n) > 20 > 20.7 \text{ for } 11(2n) \end{aligned}$$

$$\begin{aligned} \text{For } 2 < 11(2n) \\ (a_1 - b_1) > 20 > (a_2 - b_2) \\ (a_1 - b_1) > 20 > 20.7 \text{ for } 11(2n) \end{aligned}$$

which is $20.35 > 20.35$ for $11(2n)$.

$$\begin{aligned} \text{For } 2 < 11(2n) \\ 20.7 \text{ for } 11(2n) > 20 > 20.7 \text{ for } 11(2n) \\ 20.7 \text{ for } 11(2n) > 20 > 20.7 \text{ for } 11(2n) \end{aligned}$$

Summary:

- (a) For $\theta < 45^\circ$ and $\Delta E < 19.85$ kev only Cases I and II are possible.
- (b) For $\theta < 45^\circ$ and $19.85 < \Delta E < (E_L - E_C)$ only Case I is possible
- (c) For $\theta < 45^\circ$ and $19.85 < (E_L - E_C) < \Delta E$ only Cases I and V are possible.
- (d) For $\theta < 30^\circ$ and $\Delta E < 30$ kev, only cases I and II are possible.

(a) For $0 < \lambda_1 < \lambda_2$ and $\lambda_1 > \lambda_2$, we have $\lambda_1 > \lambda_2$ and $\lambda_1 > \lambda_2$.

(b) For $0 < \lambda_1 < \lambda_2$ and $\lambda_1 > \lambda_2$, we have $\lambda_1 > \lambda_2$ and $\lambda_1 > \lambda_2$.

(c) For $0 < \lambda_1 < \lambda_2$ and $\lambda_1 > \lambda_2$, we have $\lambda_1 > \lambda_2$ and $\lambda_1 > \lambda_2$.

Q.E.D.

(d) For $0 < \lambda_1 < \lambda_2$ and $\lambda_1 > \lambda_2$, we have $\lambda_1 > \lambda_2$ and $\lambda_1 > \lambda_2$.

B I B L I O G R A P H Y

1. Hanson, Taschek, and Williams, Revs. Modern Phys. 21, 635 (1949)
2. S. C. Snowden and W. D. Whitehead, Phys. Rev. 90, 615 (1953)
3. T. W. Bonner and J. W. Butler, Phys. Rev. 83, 1091 (1951)
4. E. P. Wigner, Phys. Rev. 73, 1002 (1948)
5. Feshbach, Peaslee, and Weisskopf, Phys. Rev. 71, 145 (1947)
6. A. O. Hanson and J. L. McKibben, Phys. Rev. 72, 673 (1947)
7. Nobles, Day, Henkel, Jarvis, Kutarnia, McKibben, Perry, and Smith,
Revs. Sci. Inst. 25, 334 (1954)
8. Hinchey, Stelson, and Preston, Phys. Rev. 86, 483 (1952)
9. E. Segre, Experimental Nuclear Physics, John Wiley and Sons,
(New York, 1953), Vol. I, Part II, Sect. 1.
10. S. K. Allison and S. D. Warshaw, Revs. Modern Phys. 25, 779 (1953)
11. C. B. Madsen and P. Venkateswarlu, Phys. Rev. 74, 1782 (1948)
12. Herb, Snowden, and Sala, Phys. Rev. 75, 246 (1949)

TABLE I

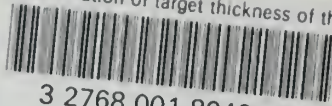
1. Hanson, James, and William, New York, 1900 (1900)
2. A. C. Hanson and V. B. Johnson, New York, 1900 (1900)
3. V. B. Johnson and A. C. Hanson, New York, 1900 (1900)
4. A. C. Hanson, New York, 1900 (1900)
5. Johnson, James, and William, New York, 1900 (1900)
6. A. C. Hanson and V. B. Johnson, New York, 1900 (1900)
7. Johnson, James, and William, New York, 1900 (1900)
8. Johnson, James, and William, New York, 1900 (1900)
9. A. C. Hanson, New York, 1900 (1900)
10. A. C. Hanson and V. B. Johnson, New York, 1900 (1900)
11. A. C. Hanson and V. B. Johnson, New York, 1900 (1900)
12. Hanson, James, and William, New York, 1900 (1900)

28803
D643 Donaghy, C. F. 28803
Determination of target
thickness of thin lithium
targets.

D643 Donaghy, C. F. 28803
Determination of target
thickness of thin lithium
targets.

thesD643

Determination of target thickness of thi



3 2768 001 89464 5

DUDLEY KNOX LIBRARY